

TPI-MINN-95-17/T; NUC-MINN-95-15/T; HEP-UMN-TH-1348

hep-lat/9505025; IPS Report 95-15; MSI Report UMSI 95/238

Submitted to Nucl. Phys. B ; Revised version, January 1996

# Determination of the renormalized heavy-quark mass in Lattice QCD

**A. Bochkarev<sup>a,†</sup> and Ph. de Forcrand<sup>b</sup>**

<sup>a</sup> *TPI, U. of Minnesota, Minneapolis, MN 55455, USA*

<sup>b</sup> *IPS, ETH-Zentrum, Zürich CH-8092, Switzerland*

Abstract

We study on the lattice the correlator of heavy-quark currents in the vicinity of vanishing momentum. The renormalized charmed quark mass, the renormalized strong coupling constant and gluon condensate can be defined in terms of the derivatives of that correlator at zero momentum. We analyze quenched Monte-Carlo data on a small lattice  $8^3 * 16$  for  $\beta = 6$ . We generalize dispersion relations to the lattice theory in a simple way and use them successfully to fit the correlator at both small and large distances. We fit the short-distance part of the correlator with the relevant expressions of perturbative QCD on the lattice and obtain the value of the renormalized quark mass  $m_c^{\overline{MS}}(m_c) = 1.20(4) GeV$ .

<sup>†</sup> On leave from: INR, Russian Academy of Sciences, Moscow 117312, Russia

# Introduction

At present the accurate calculations of the strong coupling constant  $\alpha_s$  [1] and the masses of heavy quarks [2], [3] are not only the subject of intensive studies in the continuum QCD. Monte-Carlo Lattice simulations seem to provide us with competitive ways to evaluate  $\alpha_s$  [4],[5] and heavy-quark masses [8] with considerable accuracy. A systematic study of the correlator of heavy-quark currents  $\Pi(q^2)$  near zero momentum  $q^2 = 0$  on the lattice was suggested recently [9] as a way to calculate the renormalized parameters of perturbative QCD, the strong coupling constant  $\alpha_s$  and heavy quark mass  $m_c$ , as well as the main parameter of non-perturbative QCD, the vacuum gluon condensate  $G^{(2)} \equiv \langle 0 | (\alpha_s/\pi) G_{\mu\nu}^a G_{\mu\nu}^a | 0 \rangle$  [10].

In this paper we formulate the method in more details and analyze Monte-Carlo data on relatively small lattice  $8^3 \times 16$ , as a *pilot* study. We concentrate on the renormalized mass of the charm quark  $m_c$ . The renormalized parameters of the QCD Lagrangian,  $\alpha_s(\mu^2)$  and  $m_c(\mu^2)$  serve as the boundary conditions to the renormalization group equations. Here  $\mu^2$  is some physical normalization point, which stays finite as the cut-off is removed, say the lattice spacing  $a \rightarrow 0$ . This choice of a physical normalization point allows one to easily make use of phenomenological data in the determination of  $\Lambda_{QCD}$  and current quark masses on the Lattice. It also helps to isolate such non-perturbative quantities as the gluon condensate, whose naive definition would imply a strong power-like dependence on the normalization point [11]. This is the main difference between the proposal [9] and the works [12] where the computation of the gluon condensate on the lattice was pioneered.

Because of the *asymptotic freedom* the boundary conditions to the renormalization group equations in QCD should be imposed at large Euclidean momenta corresponding to small space-like distances. The renormalized parameters of QCD are essentially the

short-distance quantities. We would like to emphasize the difference between the pole-mass of quarks and Euclidean quark mass. The pole mass is a parameter of the on-shell-subtraction scheme: the ultraviolet singularities are subtracted on the quark mass-shell. This scheme does not appeal because of the complicated infrared properties of QCD: quarks do not exist on the mass-shell. The pole mass of quarks is well defined only within the first orders of perturbation theory, while the Euclidean mass is defined in the domain where perturbative QCD applies. In the popular these days language one would say that the pole-mass suffers from the infrared-renormalon ambiguities while the Euclidean mass does not.

One way to calculate the Euclidean mass on the lattice was considered in [7]. The prescription is: *a)* within the lattice theory calculate the pole mass  $m^*$  of the quark propagator as a function of the parameters of the lattice theory  $m^*[\kappa, r, \beta, \dots]$  perturbatively in powers of the inverse bare coupling constant  $\beta$ . Here :  $\beta = 6/g^2$  and  $\kappa, r$  are parameters of the Wilson propagator. This perturbative expansion is good at large  $\beta$ , where the asymptotic scaling holds: the function  $g^2(a)$  solves the perturbative renormalization group equation. Volume has been always considered infinite in these analytic calculations. The essential ingredient of this calculation is the bare quark mass  $m(a)$ , which is obtained by fitting the Monte-Carlo data for the pion mass  $m_\pi$  with the ansatz:  $m(a) = (1/\kappa - 1/\kappa_{cr})/2$ . The motivation for this fit is that  $m_\pi^2 \sim m_{quark}$  is expected in the chiral limit. The fit is done for  $\kappa$ s corresponding to light fermions in the finite volume and for relatively small  $\beta$ s, where  $\beta$  does not scale. *b)* Use the relation of the continuum theory between the quark pole mass and the Euclidean mass  $m^*[m(\mu), \alpha_s(\mu)]$ .

Our approach is somewhat alternative to [7]. We use the correlator of hadronic currents of heavy quarks to determine the Euclidean quark mass. We never refer to the pole mass. The correlator of the heavy-quark currents is reliably calculated in perturbative

QCD at vanishing momentum, because that point is away from the nearest threshold due to heavy quark-antiquark pair production. The heavy-quark threshold  $4m_c^2$  is the relevant virtuality here. The perturbative loop-expansion is built in powers of small parameter  $\alpha_s(4m_c^2)$ . *One* loop of free quarks with the renormalized Euclidean mass gives a very good approximation to the correlator of the charm-quark currents near vanishing momentum [10]. This is in contrast to the correlator of light quarks, which is not analytic at vanishing momentum and cannot be computed at that point within perturbative QCD.

The correlator of the gauge-invariant local hadronic currents  $\Pi(x)$  is a very conventional thing to study in Lattice QCD. The long-distance behavior of the correlator is determined by the low-lying resonance. To obtain the resonance mass one fits the zero-momentum correlator  $\Pi(t)$  by  $\cosh[(t - L/2)m_{res}]$ , which describes propagation of a single particle of mass  $m_{res}$  in a finite volume  $L$  in the continuum theory ( $a = 0$ ). We do the same thing: fit the long-distance part of the correlator of heavy-quark currents with the single-resonance approximation to that correlator. This allows us to fix the scale of our Monte-Carlo data. In addition to that we study the short-distance part of the correlator as well. We fit it with the corresponding expressions of perturbative QCD in order to extract the fundamental parameters of perturbative QCD: the renormalized quark mass and the strong coupling constant.

In order to separate the short-distance part of the correlator from its long-distance part we study derivatives of the correlator  $\Pi(q^2)$  with respect to momentum  $q^2$  at the origin  $q^2 = 0$ , called moments [10]. The lower derivatives probe the vicinity of the origin, which is  $4m_c^2 \text{ GeV}^2$  away from the charm quark-antiquark threshold, hence it is in the domain of asymptotic freedom. The lower moments are reliably computed in perturbative QCD. We use Monte-Carlo data for the lower moments to extract the parameters of perturbative QCD. Higher moments probe the values of  $q^2$  away from the origin. They represent the

long-distance part of the correlator and are entirely saturated by the low-lying resonance. We use those moments in order to fix the scale of the lattice theory.

The next section 1.1 is a short introduction into the so-called dispersion theory of charmonium [11]. We describe analytic properties of the two-point correlator of charm-quark currents in the continuum theory and explain why it is reliably calculated near vanishing momentum in perturbative QCD. The other sections are our attempt to extend the dispersion theory of charmonium to the Lattice QCD.

In section 1.2 we discuss an extension of the dispersion relations to the lattice theory. Since we deal with the lattice theory of heavy quarks significant cutoff effects are expected. At  $\beta = 6$  the lattice spacing  $a \sim (2 \text{ GeV})^{-1}$ . For the charm quark mass  $m_c \approx 1.3 \text{ GeV}$  one has the parameter of the deviation of the fermionic action from the continuum  $a \cdot m_c \approx 0.6$  - moderately, but not comfortably small. Actually one would like to probe virtualities  $\mu^2 \sim 4m_c^2$  on the lattice, then  $a \cdot \mu \sim O(1)$ . From the phenomenological point of view we are trying to generate a resonance of mass  $\sim m_{J/\psi} \simeq 3.1 \text{ GeV}$ . Then the resonance mass in the units of the lattice spacing  $a \cdot m_{res} \approx 1.5$ . Such lattice theory is obviously coarse enough to exhibit certain cutoff effects in the propagation of a single resonance. We explore the cutoff effects via fitting Monte-Carlo data with the following generalization of the dispersion relation for the two-point correlator  $\Pi(q^2)$  to the lattice theory:

$$\int ds \frac{\rho(s)}{s + q^2} \implies \int ds \frac{\rho(s, a, L)}{s + \frac{4}{a^2} \sum_{\mu} \sin^2(q_{\mu} a/2)} \quad (1)$$

where  $L$  represents the finite volume of the box, and the function  $\rho(s, a, L)$  approaches the corresponding spectral density of the continuum theory in the limit  $a \rightarrow 0$ ,  $L \rightarrow \infty$ . We find significant evidence that although the l.h.s. of (1) exhibits strong deviations due to  $a \neq 0$  &  $L \ll \infty$ , the dependence of the spectral density on  $a$  and  $L$  is rather weak on the lattice under consideration. In other words, most of the cutoff effects in the heavy-quark systems are successfully taken into account by the naive modification of the denominator

in (1).

In section 2 we compare the moments of the correlator in a single-resonance approximation on the finite lattice and in the continuum theory. We compare the fit based on the dispersion relation (1) with the traditional fit to  $\cosh[(x - L/2)m_{res}]$  for different values of the parameter  $a \cdot m_{res}$ . We analyze Monte-Carlo data obtained on a blocked lattice  $8^3 \times 16$  with  $a^{-1} \simeq 500 \text{ MeV}$ , which is supposed to show correctly the long-distance part of the correlator, where the single resonance dominates. We find perfect fit to the data with help of eqn.(1) using one fit-parameter, the resonance mass:  $\rho(s) \equiv \delta(s - m_{res}^2)$ .

In order to see the manifestation of the short-distance phenomena, we have generated Monte-Carlo configurations on a small (unblocked)  $8^3 \times 16$  lattice at  $\beta = 6$ , corresponding to  $a^{-1} \sim 2 \text{ GeV}$ . We use quenched propagators of the clover- and tadpole-improved Wilson fermionic action. We find that the long-distance part of the correlator (higher moments) is still well fitted with a single resonance. We reproduce the masses of the pseudoscalar ( $\eta_c$ ), vector ( $J/\psi$ ) and scalar ( $\chi_{co}$ ) mesons of the charmonium spectrum with quite reasonable accuracy. For lower moments ( $\sim$  short-distances) though, Monte-Carlo data deviate from the single-resonance curve. However, that deviation proves to be described very well by the contribution of the excited states - a smooth hadronic continuum spectrum, which we incorporate via the dispersion relation (1).

In section 3 we study the lower moments of the correlator, corresponding to the short-distance physics. They must be reliably reproduced in perturbative QCD, which means that *one*-loop of free quarks gives the dominant contribution. The mass of those quarks is the renormalized heavy-quark mass by construction. Since there is a reliable loop expansion for the lower moments of the correlator of heavy-quark currents one can study systematic deviations of the coefficients of that expansion order by order.

First, we fit the Monte-Carlo data for the lower moments by the correlator composed

of free Wilson quark propagators. Those propagators correspond to the quarks of mass  $m_c = 1.37\text{GeV}$  in the continuum theory. To be more accurate we study a relation between the mass of the free Wilson action and the corresponding fermion mass of the continuum theory in the finite volume because the Monte-Carlo is done in the finite (and relatively small) volume. Again, we find evidence that the dispersion relation (1) works well, this time - for the continuum spectrum of quark-antiquark pair. To specify the subtraction scheme of the renormalized quark mass we take into account the two-loop  $\alpha_s$ -correction. With this refined treatment we obtain in the minimal subtraction scheme  $m_c^{\overline{MS}}(m_c) = 1.22(2)\text{GeV}$  from the vector channel and  $m_c^{\overline{MS}}(m_c) = 1.18(2)\text{GeV}$  from the pseudoscalar channel. We attribute the difference in these two values to the absence of scaling on the given lattice.

# 1 Correlator of the heavy-quark currents

## 1.1 Dispersion theory of charmonium

Consider the correlator of vector currents of charmed quarks:

$$\Pi(q^2)_{\mu\nu} = i \int dx e^{iqx} \langle 0 | T \{ j_\mu(x) j_\nu(0) \} | 0 \rangle \quad (2)$$

where  $j_\mu = \bar{c} \Gamma c$ . The correlator (2) in the continuum theory satisfies the standard dispersion relation:

$$\Pi(q^2)_{\mu\nu} = (q_\mu q_\nu - g_{\mu\nu} q^2) q^2 \int ds \frac{\rho(s)}{s^2(s + q^2)} + d_1 g_{\mu\nu} + d_2 (q_\mu q_\nu - g_{\mu\nu} q^2) \quad (3)$$

The correlator  $\Pi(q^2)_{\mu,\nu}$  is defined up to the polynomial, which coefficients  $d_{1,2}$  have ultra-violet singularities. The polynomial with the coefficients  $d_1$  and  $d_2$  is a local part of the correlator. In the  $X$ -space one has:

$$\Pi(x)_{\mu\nu}^{local} = d_1 g_{\mu,\nu} \delta^{(4)}(x) + d_2 (\partial_\mu \partial_\nu - g_{\mu\nu} \partial^2) \delta^{(4)}(x) \quad (4)$$

$j_\mu$  is essentially electromagnetic current of charmed quarks. The correlator (2) describes electromagnetic vacuum polarization due to strong interactions. The coefficient  $d_1$  renormalizes photon mass, while the coefficient  $d_2$  renormalizes photon wave function. If the ultraviolet singularities are subtracted on the photon mass shell  $q^2 = 0$  one has  $d_1 = d_2 = 0$  for the renormalized correlator.

The spectral density  $\rho(s)$  is proportional to the inclusive cross-section of the production of charmed and anticharmed hadrons in  $e^+e^-$ -annihilation via the electromagnetic current of heavy quarks. From experiment one knows that  $\rho(s)$  has a large peak due to  $J/\psi$ -meson. Higher radial excitations with smaller contribution to the spectral density overlap with the continuum spectrum of multiparticle states. The simple and phenomenologically very successful ansatz for  $\rho(s)$ :

$$\rho_{phen}(s) = s \left( f m_{res}^2 \delta(s - m_{res}^2) + \frac{1}{4\pi^2} \theta(s - s_o) \right) \quad (5)$$

contains a single low-lying resonance of mass  $m_{res} = m_{J/\psi}$ , residue  $f$ , proportional to the electromagnetic width of the  $J/\psi$ -meson and a smooth continuum spectrum with some effective threshold  $s_o > m_{res}^2$ . The coefficient  $1/4\pi^2$  comes from one loop of free quarks. The fact that continuum hadronic spectrum at high energies  $s > s_o$  is identical to the perturbative spectrum of free quarks (with small radiative corrections) is usually referred to as *global duality* [13]. This property is a consequence of asymptotic freedom.

Since the poles and discontinuity of the correlator  $\Pi(q^2)_{\mu\nu}$  are located away from the origin  $q^2 = 0$  the correlator is analytic at  $q^2 = 0$ . Following [10] define moments of the polarization operator (2) as:

$$\mathcal{M}_n = \frac{1}{n!} \left\{ \left( -\frac{d}{dq^2} \right)^n \Pi_{\mu\mu}(q^2) \right\}_{q^2=0} \quad (6)$$

From the spectral representation (3) one obtains:

$$\mathcal{M}_n = -3 \int ds \frac{\rho(s)}{s^{n+1}} \quad (7)$$



Obviously the first two moments  $\mathcal{M}_{0,1}$  suffer from ultraviolet singularities whereas all the other moments are physical quantities: the ultraviolet singularities in them can be absorbed via the renormalization of the Lagrangian parameters, the strong coupling constant and the charmed quark mass.

The quantity we study below is the ratio  $r_n$  of the neighboring moments:  $r_n = \mathcal{M}_{n+1}/\mathcal{M}_n$ . The phenomenological spectrum (5) has the following ratios

$$\begin{aligned} r_n &= \frac{1}{m_{res}^2} \frac{\eta_n}{\eta_{n-1}}, \\ \eta_n &\equiv 1 + \frac{1}{4\pi^2 n f} \left( \frac{m_{res}^2}{s_o} \right)^n \end{aligned} \quad (8)$$

One can see that the continuum contribution to the higher moments rapidly decreases. Higher moments are saturated by large distances, where the single low-lying resonance dominates. The ratios (9) corresponding to the single-resonance approximation to the correlator (2) are particularly simple:

$$r_n^{res} = \frac{1}{m_{res}^2} \quad (9)$$

where  $m_{res}$  stands for the resonance mass. This is illustrated in Fig.1.

Lower moments receive substantial contribution from the continuum spectrum. They probe the vicinity of the origin  $q^2 = 0$ . From the QCD point of view that region is in the domain of asymptotic freedom: the nearest threshold due to a pair of charmed quark and antiquark is away by  $4m_c^2 \gg \Lambda_{QCD}^2$ .

The function  $\Pi(q^2)$  is reliably calculable in perturbative QCD near  $q^2 = 0$ . Low-energy thresholds due to multi-gluon intermediate states, which appear on the 4-loop level, are known to give small contributions in the case of heavy quarks [10]. They may be eliminated altogether by giving different masses to the two quarks of the current.  $\Pi(q^2 = 0)$  is a function of the renormalized heavy quark mass  $m_c(\mu)$  and  $\alpha_s(\mu)$ . The relevant renormalization point here,  $\mu = 2m_c$ , is high enough to ensure the validity of

the QCD perturbation theory:  $\alpha_s(4m_c^2) \simeq 0.2$ . Then the applicability of perturbative QCD near  $q^2 = 0$  implies the following expansion for the ratios  $r_n$ :

$$r_n = \frac{1}{4m_c^2} \left( a_n + b_n \alpha_s(4m_c^2) - c_n \frac{G^{(2)}}{(4m_c^2)^2} \right) \quad (10)$$

where  $\{a_n, b_n, c_n\}$  are known numbers [10]. The term  $\sim a_n$  comes from one loop of free charmed quarks. The term  $\sim b_n$  comes from the two-loop diagrams corresponding to one-gluon exchange. The gluon condensate  $G^{(2)} \equiv \langle 0 | (\alpha_s/\pi) G_{\mu\nu}^a G_{\mu\nu}^a | 0 \rangle$  is the vacuum average of the first nontrivial operator in the Wilson operator-product expansion for the correlator of heavy-quark currents. The coefficient  $c_n$  originating from the Wilson coefficient function starts with one loop of the heavy-quark propagators.

The lower ratios  $r_{2,3,4}$ , originating from short distances, are well reproduced by QCD perturbation theory. The typical virtuality corresponding to the  $n$ th moment is  $\sim 4m_c^2/n$ . The coefficient  $b_n$  grows with  $n$ . At large  $n > 8$  the perturbation-theory based expansion (10) is irrelevant. The gluon condensate shows up in the intermediate ratios  $r_{5,6,7}$  [10], sensitive to larger distances and, hence, nonperturbative fluctuations. It represents the first term of the operator product expansion. The operator-product expansion thus describes a crossover from the short-distance region to the large-distance region, in the vicinity of the domain of asymptotic freedom. The contribution of the gluon condensate into the physical quantity  $r_n$  is renormalization-scale independent. To extract the value of the gluon condensate from  $r_n$  one has to know the parameters of perturbative QCD. The better one knows  $\alpha_s$  and  $m_c$  from the lower moments  $r_{2,3,4}$  - the higher the accuracy that can be reached in the calculation of the gluon condensate from  $r_{5,6,7}$ .

The phenomenological parameters of hadronic spectrum (5), based on experimental data on the inclusive cross-section of charm-anticharm production in  $e^+e^-$ -annihilation, are :

$$4\pi^2 f \simeq 0.6, \quad m_{res} \simeq 3.1 \text{ GeV}, \quad s_o \simeq (4 \text{ GeV})^2 \quad (11)$$

The moment ratios of the corresponding correlator are shown on Fig. 1. One can see that the higher moments  $n \geq 7$  of the complete correlator, shown by bursts, coincide with the single-resonance approximation to that correlator - the contribution of the  $J/\psi$ -meson, shown by squares. The lower moments, corresponding to the short-distance part of the correlator, deviate from the single-resonance line. They are well reproduced with one loop of free quarks of mass  $m_c = 1.26 GeV$ , which moment ratios are shown by diamonds. This way the mass of charmed quark was first estimated within QCD in [10].

In order to make this estimate more accurate one has to know the contribution of continuum hadronic spectrum very well, since it is large in the lower moments. However, this is demanding with respect to experimental data on the inclusive cross-section of charm-anticharm production in the  $e^+e^-$ -annihilation. Additional uncertainty here is due to the fact that at high energies one has to separate the bigger part of that inclusive cross-section, coming from the electromagnetic current of heavy quarks, from the smaller part of that cross-section, coming from the electromagnetic current of light quarks. In order to avoid the uncertainty associated with the hadronic continuum alternative ways to determine charmed quark mass have been developed. They are based on the nonrelativistic approximation to QCD. Potential models [3] are particularly successful for  $b$ -quarks. Charmed quarks are light enough to exhibit substantial relativistic effects. In this work we choose to stay within the original QCD rather than to study nonrelativistic approximations to it. In order to avoid the uncertainty due to hadronic continuum we evaluate the correlator (2) by Monte-Carlo in lattice theory. The lattice calculation requires much less experimental data. One only has to know the mass of the low-lying resonance in order to fix the scale of the lattice theory.

The fact that the lower moments are well reproduced in perturbative QCD implies an integral relation, called *sum rule*, between the parameters of perturbative QCD and

phenomenological parameters of hadronic spectrum:

$$\int \frac{ds}{s^{n+1}} \rho_{QCD}(s) = \int \frac{ds}{s^{n+1}} \rho_{phen}(s) \quad (12)$$

where  $n = \{2, 3, 4\}$  and  $\rho_{QCD}(s)$  is the spectral density corresponding to the multiloop expansion of perturbative QCD (10). The parameters of hadronic spectrum, consistent with the sum rule (12) and experimental data (available in the case of vector channel), are those in eqn.(11).

One important implication of the sum rules (12) is that smooth hadronic continuum spectrum, which form coincides with the corresponding perturbative expression, *must* be incorporated in the model of the hadronic spectral density. At high energies the continuum spectrum dominates over the contribution of few excited states. The high-energy asymptotics of the hadronic spectrum must be the same as predicted by the perturbative QCD. Therefore, a finite number of narrow resonances is ruled out as a model of hadronic spectral density of the correlator (2).

One should emphasize that light quarks do not participate in the derivation of the spectrum (11) in a sense that the expansion (10) does not contain diagrams with light quarks. Incorporation of light quarks would bring more accuracy, in general, but the contribution of light quarks into the lower moments is essentially small, as they appear in higher orders of the reliable perturbative expansion in powers of  $\alpha_s(4m_c^2)$  [10].

## 1.2 Dispersion relation on the lattice

In the previous section we have pointed out that the short-distance part of the correlator ( $r_{2,3,4}$ ) receives substantial contributions from the high-energy (continuum) part of the spectrum. When analysing the data on the correlator in lattice QCD we would like to know how the correlator with a given spectrum looks like in the lattice theory. How the

finite volume and finite cutoff modify the function  $\Pi(x)$  with the spectral density as in (5)?

We explore the following naive extension of the dispersion relation (3) to the lattice theory:

$$\Pi(q_\mu, a, L) = \int ds \frac{\rho(s, a, L)}{s + \frac{4}{a^2} \sum_\mu \sin^2(q_\mu a/2)} \quad (13)$$

In principle, one should expect the spectral density in (13) to have lattice artifacts. In practice we find that the simple modification of the denominator as in (13) accounts for the major part of systematic deviations due to finite  $L$  and  $a$ . Eqn.(13) allows one to fit Monte-Carlo data by a complicated spectrum with several resonances and a smooth continuum.

In the case of a single resonance  $\rho(s) = \delta(s - m_{res}^2)$  eqn.(13) becomes a familiar expression for the lattice propagator of a free field:

$$\Pi^{res}(q^2, \mathbf{n}) = \frac{1}{m_{res}^2 + \frac{4}{a^2} \sum_\mu \sin^2(q_\mu a/2)} \quad (14)$$

where we have introduced a four-vector  $\mathbf{n}$  of unit length:  $q_\nu \equiv q n_\nu$ , so that  $\sum_{\nu=1}^4 n_\nu^2 = 1$ .

The extra dependence of the correlator on  $n_\nu$  is an  $\mathcal{O}(a^2)$ -effect.

To see how well eqn.(13) works for the continuum spectrum we fit in section 3 the lattice correlator in the free Wilson quarks approximation (which has continuum spectrum) to the eqn.(13) with the quark-antiquark spectral density of the continuum theory. It proves to work well on finite lattices of different size.

Since we are interested in the short-distance behavior of the correlator we have to address the question of subtractions. At short distances the correlator is singular. In the continuum theory the ultraviolet singularities are proportional to the polynomial of finite order in the momentum space. The finite order of that polynomial is a consequence of the renormalizability of the theory. The renormalized correlator is the one with the

infinite parts of the local terms subtracted. In the continuum theory the difference between subtracted and unsubtracted correlator is polynomial in  $q^2$ . For example, in the correlator of the vector currents (2) that polynomial is quadratic:  $d_1 + d_2 q^2$ . The factor  $q^2$  here is essentially the inverse Laplacian of the continuum theory. The subtraction polynomial contributes only to the first two moments. The other moments do not receive any contribution at all from the subtraction polynomial.

Let us see what the difference is between the subtracted and unsubtracted lattice dispersion relation (13). The subtraction:

$$\frac{1}{s + \frac{4}{a^2} \sum_{\mu} \sin^2(q_{\mu} a/2)} - \frac{1}{s} = - \frac{\frac{4}{a^2} \sum_{\mu} \sin^2(q_{\mu} a/2)}{s \left( s + \frac{4}{a^2} \sum_{\mu} \sin^2(q_{\mu} a/2) \right)} \quad (15)$$

generates non-polynomial terms  $q_{lat}^2 \equiv \frac{4}{a^2} \sum_{\mu} \sin^2(q_{\mu} a/2)$  instead of  $q^2$  in the numerator.

To perform a subtraction in the lattice theory one would have to decompose the correlator (13) in the following form:

$$\begin{aligned} \Pi(q^2) &= \tilde{d}_1 + \tilde{d}_2 \frac{4}{a^2} \sum_{\mu} \sin^2(q_{\mu} a/2) \\ &+ \left( \frac{4}{a^2} \sum_{\mu} \sin^2(q_{\mu} a/2) \right)^4 \int ds \frac{\rho(s)}{s^2 \left( s + \frac{4}{a^2} \sum_{\mu} \sin^2(q_{\mu} a/2) \right)} \end{aligned} \quad (16)$$

The factor  $q_{lat}^2$  is the inverse of the standard lattice Laplacian:

$$\int \frac{d^4 q}{(2\pi^4)} e^{iqx} \frac{4}{a^2} \sum_{\mu} \sin^2(q_{\mu} a/2) = (2\delta(x) - \delta(x-a) - \delta(x+a)) / a^2 \quad (17)$$

Therefore the coefficient  $\tilde{d}_2$  in (16) is precisely the renormalization of the photon wave function in the case of vector currents of charmed quarks. The renormalized correlator would be given by eqn.(16) with  $\tilde{d}_1 = \tilde{d}_2 = 0$ , considered as a function of the renormalized Lagrangian parameters.

The deviation of the  $q_{lat}^2$ -term from a polynomial  $q^2$  is an  $\mathcal{O}(a^2)$ -cutoff effect. It generates  $\mathcal{O}(a^n)$  systematic deviations in the moments, which decrease rather fast with

$n$ . For a single resonance, for example, in the 1-dimensional case one can find analytically explicitly:

$$\mathcal{M}_n^{res} = \left\{ 1 + \frac{n!}{(2n)!} (am_{res})^n \right\} \frac{1}{(am_{res})^{2n}} \quad (18)$$

In the next sections we will see the size of the contribution of the subtraction term  $q_{lat}^2$  into the moments on finite lattices. The ratios  $r_n$  for  $n \geq 3$  prove to be practically not affected by subtractions.

## 2 Moments on a finite lattice

### 2.1 Single resonance

The definition of the moments (6) is designed in such a way that the ratios  $r_n$  of the neighboring moments of the correlator, saturated by a single resonance, are all equal to the inverse mass squared of that resonance. This suggests a simple way to determine the resonance mass numerically from given data on the correlator (2). The property (9) however, holds in the continuum theory, that is in the limit  $a \rightarrow 0$  and  $L \rightarrow \infty$ . One has to see how much the moments of a single resonance are distorted by the finite  $L$  and  $a$ .

The extension of the definition of moments (6) to the case of a finite lattice (with broken Lorentz invariance) was suggested in [9]:

$$\mathcal{M}_n = \frac{1}{2^{2n} n!(n+1)!} \int dx^4 x^{2n} \Pi(x) \quad (19)$$

In the continuum theory eqns. (6) and (19) are identical. An alternative to (19) would be to project the correlator (2) to  $\vec{q} = 0$  and define the moments as derivatives with respect to  $q^0$ . In this work we explore the Lorentz invariant definition (19).

We have evaluated the moments (19) of a single resonance (14) numerically on a given lattice. Figs. 2,3,4 show the moments of a single resonance for different volumes. One can

see very strong finite volume effects. For small values of  $L$  and  $am_{res}$  the moments are far away from the straight line (9) of the continuum theory, illustrated by squares in Fig.1. As one increases the volume, the moments approach a straight line corresponding to (9). This works better for larger values of  $am_{res}$  (Fig.4), corresponding to more compact resonance-objects. The constant behavior of  $r_n$  is clearly seen for  $m_{res} = 1.5$  in the whole range of the ratios of interest  $r_{1\div 7}$  on a large lattice  $32^4$ . For larger  $n$  the moments deviate from the prediction of the continuum theory (9) because higher moments probe larger distances, hence they are more sensitive to the boundary of the box. Figure 5 shows the behavior of the moments for different resonance masses  $m_{res} = 0.5 \div 2$  on the lattice  $16^3 * 32$ . Again, one can see that finite-volume effects disappear for larger values of the resonance mass in the units of the lattice spacing. It is important to realize that these finite-size effects do not represent any loss of information. The curves are universal and may (will) be used to fit Monte-Carlo data on the same lattices.

Figs. 2,3,4 show the moments of the subtracted correlator as well. The subtracted correlator has vanishing first two moments  $\mathcal{M}_{0,1} = 0$ . The ratio  $r_1 = \mathcal{M}_2/\mathcal{M}_1$  of the subtracted correlator is not to be considered. The two solid lines on Figs. 2, 3, 4, corresponding to the subtracted and unsubtracted correlators, are indistinguishable except for the second ratio  $r_2$ . The line corresponding to the subtracted correlator is always the one that terminates at  $n = 2$ . In the continuum theory the ratio  $r_2$  is not affected by subtractions because the subtraction polynomial is  $O(q^2)$ . On the lattice the subtraction term  $q_{lat}^2$  gives contributions to higher moments. Those contributions are noticeable in the ratio  $r_2$  and negligible in higher ratios. The deviation between the subtracted and unsubtracted curve in the ratio  $r_2$  is order  $O(a^2)$  effect. One can see that the deviation in the ratio  $r_2$  decreases with the resonance mass, because the decrease in the resonance mass here essentially implies the decrease in the lattice spacing  $a$ . In the limit  $a \rightarrow 0$  one



has  $q_{lat}^2 \rightarrow q^2$ , hence the ratio  $r_2$  becomes insensitive to subtractions.

Concentrating on the cutoff effects we extract the resonance mass from the ratio  $r^* \equiv r_n(L \rightarrow \infty)$ , observed on the biggest available lattice  $32^4$ , by looking for a plateau like the one on the upper curve of Fig. 4 for  $n < 8$ . Increasing the volume would extend this plateau to larger  $n$ , while its position would not change. This would be our procedure to fit the resonance mass  $\bar{m}_{res} \equiv (r^*)^{-1/2}$  via the analysis of the moments. However, even if the lattice is large enough to exhibit a perfect plateau for  $r_n = r^*$ , corresponding to the continuum theory, the position of that plateau gives  $1/m_{res}^2$  only approximately because of finite- $a$  effects, as one can notice by inspecting the upper lines of Figs. 3 and 4. The resonance masses  $\bar{m}_{res}$  are plotted on Fig. 6 versus the input mass  $m_{res}$ . The fit of that data gives the following  $\mathcal{O}(a^2)$ -systematic deviation<sup>1</sup>:

$$\frac{1}{\bar{m}_{res}^2} = \frac{1 + 0.04 m_{res}^2}{m_{res}^2} \quad (20)$$

The fluctuations of the data Fig. 6 around the fit (20) near  $m_{res} = 1$  are caused by our uncertainty in determining the plateau  $r_n = r^*$ , which is not well-established yet on a  $32^4$ -lattice for those values of  $m_{res}$ . The value  $m_{res} = 3$  is obviously too large to be fitted by the  $\mathcal{O}(a^2)$ -law (20). The systematic correction (20) is rather small for  $m_{res} \leq 1$ , so the present Monte-Carlo data for light quarks (where the resonance masses in units of the lattice spacing are typically less than 1) does not see it.

In Fig. 7 we compare the resonance mass  $\bar{m}_{res}$  with the conventional way of extracting the resonance mass from the correlator (2) - a fit to  $\cosh(t - L/2)$  at vanishing three-dimensional momentum  $\vec{q} = 0$ . One can see that the resonance mass  $\bar{m}_{res}$ , extracted from the moments is always a better approximation to the expected result  $m_{res}$ .

---

<sup>1</sup> All the dimensional quantities in the lattice theory are in units of the lattice spacing  $a$  throughout this paper, although we show the factor  $a$  explicitly sometimes to draw attention to the dependence on it.

## 2.2 Monte-Carlo data

In this section we analyze the moments of the correlator (2), computed by Monte-Carlo in the quenched approximation, first on a large but coarse lattice obtained by blocking, then on a small but fine lattice. These two studies allow us to check separately our numerical control of large and small moments.

The fermionic action we use  $S_F = S_W + S_{SW}$  has the Wilson term  $S_W$  and the clover term  $S_{SW}$  [19]:

$$S_W = \sum_x \{ \bar{\psi}(x) \psi(x) - \kappa_W \sum_{\mu} [ \bar{\psi}(x)(r - \gamma_{\mu})U_{\mu}(x)\psi(x + \hat{\mu}) + \bar{\psi}(x + \hat{\mu})(r + \gamma_{\mu})U_{\mu}^{\dagger}(x)\psi(x) ] \} \quad (21)$$

$$S_{SW} = - \frac{r \kappa_W}{2} c \sum_{x, \mu, \nu} \bar{\psi}(x) F_{\mu\nu}(x) \sigma_{\mu\nu} \psi(x) \quad (22)$$

where  $F_{\mu\nu}$  is a field-strength tensor as the following sum of four plaquettes in the  $\mu\nu$  plane around point  $x$ :

$$F_{\mu\nu}(x) = \frac{1}{8} \sum_{\square=1}^4 [ U_{\square\mu\nu}(x) - U_{\square\mu\nu}^{\dagger}(x) ] \quad (23)$$

The action  $S_F$  does not have terms of order  $O(a)$  in the expansion in powers  $a$  as  $a \rightarrow 0$  for  $c = 1$  [19]. The Green functions computed with the help of action  $S_F(c = 1)$  do not differ from their limit  $a \rightarrow 0$  in the order  $O(a)$  provided the fermionic fields  $\psi(x)$  are related to their  $a \rightarrow 0$  limit as follows:

$$\psi \rightarrow \left( 1 - \frac{ra}{2} (z\gamma_{\mu}D_{\mu} - (1-z)m^w) \right) \psi \quad (24)$$

where  $m^w$  is the bare quark mass, parameter of the Wilson propagator, and  $D_{\mu}$  is the lattice covariant derivative and  $z$  arbitrary parameter, corresponding to the possibility of using the equations of motion [20]. We choose  $z = 0$ .

However, the systematic deviations of the order  $O(g^{2n}a)$  are generated by the action  $S_F$ . With the hope to diminish them we would like to eliminate tadpole diagrams within

the mean-field approximation [16]. The tadpole diagrams make average links differ from one:  $\langle U_\mu \rangle \neq 1$ . The suggestion of [16] is to absorb these factors by the nonperturbative renormalization of the parameters of the lattice action. Identifying  $\langle U_\mu \rangle = \langle U_\square \rangle^{1/4}$  in the mean-field approximation, we divide every link in (21), (22) by  $\langle U_\square \rangle^{1/4}$ . This implies that we use a new  $\kappa = \kappa_W / \langle U_\square \rangle^{1/4}$  in  $S_F$  and nontrivial value of the coefficient  $c$  against clover term (22):  $c = \langle U_\square \rangle^{-3/4}$ .

### 2.3 Blocked lattice

We have obtained a set of blocked  $SU(3)$  configurations from the QCD-TARO collaboration [15]. Starting from a  $32^3 \times 64$  lattice at  $\beta = 6$ , corresponding to  $a^{-1} \simeq 2GeV$  [17], two blocking steps were performed. This brought the lattice size to  $8^3 \times 16$ , with a rather large lattice spacing  $a^{-1} \sim 500MeV$ . The blocking process preserves information about large distances, but of course does not allow us to study short-distance effects. In [18] the clover- [19]-and-tadpole-improved [16] quark propagators were computed on these blocked configurations. These propagators were used in [9] to evaluate the moments of the correlator of vector currents. Here we fit those moments by the moments of a single resonance computed in the same box in accordance with section 1.1.

Fig. 8 shows the moments of the correlator of pseudoscalar currents. Three sets of data correspond to three different values of  $\kappa = \{0.1111, 0.1031, 0.0983\}$ . Statistical errors are shown on the graph. The upper curve, corresponding to relatively light quarks  $\kappa = 0.1111$ , ( $m_{pion} \sim 500MeV$ ) comes from 28 configurations. The other two sets of data correspond to heavy quarks, where statistical errors become small for already  $\sim 10$  configurations. The solid lines connect the ratios of the moments of a single resonance, computed on the same lattice size  $8^3 \times 16$ . The input mass of that resonance  $m_{res}$  is a fit parameter, which we find to be:  $m_{res} = \{1.08, 1.95, 2.36\}$ . In this approach, the fitted

resonance mass automatically corrects for the systematic deviation (20). One can see that the solid lines fit the Monte-Carlo data perfectly at all points despite the nontrivial shape of the curves. (The first two ratios  $r_{1,2}$  are not to be considered because they are subject to subtractions as explained in the previous section.) This implies that the Monte-Carlo data on the correlator is saturated entirely by a single resonance, which is of no surprise: the blocked lattice sees large distances only.

## 2.4 Fine lattice

In order to be sensitive to the high-energy part of spectrum, which controls the behavior of the correlator at short distances, we have generated  $SU(3)$  Monte-Carlo configurations on a small  $8^3 * 16$ -lattice at  $\beta = 6$  ( $a^{-1} \simeq 2GeV$ ). Quark propagators were computed for the clover-and-tadpole-improved action.

Fig.9 shows Monte-Carlo data from 20 configurations for the moments of the pseudoscalar (squares), vector (octagons) and scalar (diamonds) correlators for  $\kappa = 0.1000$ . Statistical errors (shown in Fig. 9, 10, 11) are rather small because the quarks are heavy. 3000 sweeps were used for thermolization and 1000 sweeps separated configurations for decorrelation. No correlations from one configuration to the next were noticed.

We fit the higher moments  $n \geq 8$  by the moments of a single resonance, computed in an  $8^3 \times 16$  box (solid lines). Fig.9 shows three sets of double solid lines, corresponding to the three channels: pseudoscalar, vector and scalar. The lines are doubled to show the impact of statistical errors, estimated by jack-knife, on the determination of the resonance mass. The masses of the resonances in units of the lattice spacing are shown in the tables. The spectrum of the charmonium ground states thus obtained is shown in Fig.10. It is gratifying to reproduce the charmonium spectrum with such a reasonable accuracy on a small lattice  $8^3 * 16$ . Current simulations of heavy systems [4] are performed

on significantly larger lattices. The reason for this success is that the charm-anticharm bound states are small objects: the size of the  $J/\psi$ -meson is  $\sim 600\text{MeV}$ . Also the splitting between  $S$ -wave states and  $P$ -wave states has a perturbative nature within the nonrelativistic approximation, and is accounted for by the leading loop of free quarks.

The new feature that one observes in Figs. 9, 11 is that the lower moments deviate from the single-resonance curve. This was not seen at all on the blocked lattice. We attribute this fact to the short-distance contributions.

We have modelled the hadronic spectral density as in (5) with the phenomenological parameters of the charmonium spectral density (11) and computed the moments of the corresponding correlator on an  $8^3 \times 16$  lattice in accordance with (13). The phenomenologically obtained lattice moments, shown in Fig. 11 by the dashed line, fit the Monte-Carlo data perfectly. It is obviously the contribution of the high-energy part of the hadronic spectrum which accounts for the deviation of the Monte-Carlo data from the single-resonance curve at lower moments. The contribution of the continuum spectrum in the smaller ratios is obviously quite large, as it accounts for the strong deviation of the Monte-Carlo data from the single-resonance curve. In contrast to that, the continuum contribution is quite small for  $n > 6$  as compared to the resonance one. This helps to determine the resonance mass with better accuracy.

Fig. 12 compares the two ways of extracting the resonance mass from Monte-Carlo data. The upper curve shows fit to the moment ratios with the single-resonance approximation to the correlator. The curve flattens at higher moments corresponding to large distances, where the single resonance dominates. The conventional fit of the zero-momentum component of the correlator to  $\cosh[(t-L/2)m_{res}]$  is shown on Fig. 13. We do not see a wide horizontal plateau at large  $n$  on Fig. 12 (or at large  $t$  on Fig. 13) because the volume of the box  $8^3 * 16$  is small and the contribution of the high-energy part of the

spectrum is noticeable. The bottom curve on Fig. 12 takes into account the contribution of the high-energy part of the spectrum. We use ansatz (5) in the dispersion relation (13) with fixed residue of the resonance and the ratio of the effective continuum threshold to the resonance mass. Those two parameters are taken to have phenomenological values as in (11). The resonance mass then remains a fit parameter. The procedure is applied to the pseudoscalar and scalar channels with similar values of the phenomenological dimensionless spectrum parameters  $f$  and  $s_o/m_{res}^2$ . Our typical statistical error in the vector and pseudoscalar resonance masses is  $\sim \pm 1\%$ , while in the scalar channel it is  $\sim \pm 5\%$ . The values of the resonance mass obtained this way are shown in the tables. The continuum contribution helps to stabilize the resonance mass at smaller  $n$ . On bigger lattices one can probe longer distances, where the continuum contribution is very small, and obtain stable curves for the resonance mass in a wide range of  $n$  without using the continuum contribution.

The model of the spectrum at high energies in the form of a smooth perturbative continuum is, in principle, better than the two-resonances fit because this model respects the global duality, which requires that the spectral density does not decrease at high energies. In the world with no light quarks (corresponding to the quenched simulations) the smooth continuum models an infinite (in the limit of infinite cutoff) series of resonances, while in the world with light quarks the effective continuum threshold is close to the  $D-\bar{D}$ -meson pair production in the charmonium vector channel. Since the model of the smooth perturbative continuum is somewhat rough in any case, one should not consider *bad* quantities, which are very sensitive to the precise form of the continuum spectrum. *Good* quantities are those related to integrals over the spectral density of the form of eqn.(12).

The value  $\kappa = 0.1060$  reproduces  $m_{\eta_c} = 2.979 GeV$ , for the lattice spacing  $a^{-1} =$

1.90GeV, and it reproduces  $m_{J/\psi} = 3.097\text{GeV}$  for  $a^{-1} = 1.92\text{GeV}$ . These values of the lattice spacing are consistent with the string-tension measurements at  $\beta = 6$  [17]. Neighboring values of  $\kappa$  are also possible, if one changes the lattice spacing accordingly; to leading order the changes in  $\kappa$  and in  $a$  compensate each other, and our physical results on the charmonium spectrum and the charmed quark mass are not affected. The value of the mass splitting within the  $S$ -wave that we obtain with the tadpole improved clover action is  $m_{J/\psi} - m_{\eta_c} = 87 \pm 9 \text{ MeV}$ .

Fig. 11 is analogous to Fig. 1. It demonstrates the important fact that the high-energy part of the spectrum and the low-energy modes can be seen on the same lattice of limited size. In the next section we study the lower moments. We fit them with the corresponding expressions of perturbative QCD.

### 3 The renormalized heavy-quark mass

#### 3.1 Off-shell mass on the lattice

While the large-distance behavior ( $n \gg 1$ ) of the correlator (2) is dominated by a single resonance, the short-distance behavior ( $n \sim 1$ ) is determined by one-loop of heavy quarks. Since the Monte-Carlo simulation is done in the lattice theory with noticeable finite-volume and cutoff effects, we have to fit Monte-Carlo data with the loop-expansion of perturbative QCD evaluated in the lattice theory as well. In other words, we have to know the systematic deviations in the coefficients  $a_n(a, L)$ ,  $b_n(a, L)$ ,  $c_n(a, L)$  of eqn.(10). As the two-loop  $\alpha_s$ -correction is small in  $r_{2,3,4}$  we first concentrate on one loop of free quarks and clarify its systematic deviations completely.

Consider the propagator of free Wilson fermions:

$$S(q) = \frac{-i \sum_{\mu}^4 \gamma_{\mu} \sin(q_{\mu}) + r \sum_{\mu}^4 (1 - \cos(q_{\mu})) + m_c^w}{\sum_{\mu}^4 \sin^2(q_{\mu}) + [\sum_{\mu}^4 r (1 - \cos(q_{\mu})) + m_c^w]^2} \quad (25)$$

At the tree level the fermion mass  $m_c^w$  is related to the hopping parameter  $\kappa$  in a simple way:

$$am_c^w = \frac{1}{2\kappa} - 4r \quad (26)$$

The parameter  $r$  is in the interval  $0 \leq r \leq 1$ . We use the notation  $m_c^w$  to emphasize that this mass is a parameter of the lattice theory.

Evaluating numerically the moments of the correlator (2) in the free-fermions approximation (with Wilson propagators (25) for  $r = 1$ ), we obtain the ratios  $r_n$  as shown on Fig. 14 for periodic boundary conditions. Again, as in the case of the resonance, one observes a strong volume dependence: higher moments, corresponding to long distances, feel the boundary of the box. As the volume increases  $8^4 \rightarrow 32^4$  the function  $r_n$  approaches the form of the continuum theory shown in Fig. 1 by diamonds. In the continuum theory the moment ratios of vector, pseudoscalar and scalar correlators in the one-loop approximation are known to be [10]:

$$r_n^{vec} = \frac{n^2 - 1}{n^2 + 3n/2} \frac{1}{4\bar{m}_c^2}, \quad (27)$$

$$r_n^{psc} = \frac{n - 1}{n + 1/2} \frac{1}{4\bar{m}_c^2}, \quad (28)$$

$$r_n^{sca} = \frac{n - 1}{n + 3/2} \frac{1}{4\bar{m}_c^2} \quad (29)$$

with the universal property:

$$r_{n \rightarrow \infty} \rightarrow \frac{1}{4\bar{m}_c^2} \quad (30)$$

where  $\bar{m}_c$  is the tree-level quark mass in the continuum theory. On Fig. 15 we compare the numerically computed moments of the pseudoscalar correlator for free Wilson quarks on the  $32^4$  lattice for  $\kappa = 0.1$ , ( $m_c^w = 1$ ) (solid line) with the corresponding values of the



continuum theory (28) (diamonds) for  $\bar{m}_c = 1$ . The discrepancy between the solid line and the diamonds is too large to remain unexplained. The asymptotics of the solid line at large  $n$ , determined by the large-distance ( $q \rightarrow 0$ ) behavior of the correlator, deviates from (30). To understand this we explore the fermion propagator (25) at small momenta. In the limit  $q \rightarrow 0$  one finds the following behavior of the denominator in (25):

$$\sum_{\mu}^4 \sin^2(q_{\mu}) + \left[ \sum_{\mu}^4 r (1 - \cos(q_{\mu})) + m_c^w \right]^2 \rightarrow q^2 (1 + r \cdot m_c^w) + (m_c^w)^2 \quad (31)$$

One can see here the lattice renormalization of the fermion wave-function  $\sqrt{1 + ram_c^w}$ , reported previously [16], as well as the following tree-level lattice renormalization of the fermion mass:

$$r_{n \rightarrow \infty} \rightarrow \frac{1}{4(a\bar{m}_c)^2} = \frac{1}{4(am_c^w)^2} (1 + ram_c^w) \quad (32)$$

Eqn. (32) is  $\mathcal{O}(a)$  systematic deviation. The fermion mass of the continuum theory is related to  $\kappa$  in a way more complicated than (26) even at the tree level. The ratios  $r_n$  of the continuum theory corresponding to  $\bar{m}_c(m_c^w = 1)$  are shown in Fig. 15 by the dashed line. Deviation of the solid line from the dashed line at  $n \sim 10$  is a finite-size effect, which would disappear on lattices larger than  $32^4$ . The equality of the asymptotics ( $n \rightarrow \infty$ ) of the solid line and the dashed line is expected by construction. The remarkable overlap between the solid and dashed lines over a wide range of  $n$  is less trivial. It means that the correlator (2) composed of free Wilson fermions behaves as in the continuum theory over a wide range of distances, provided the relation (32) between the masses  $\bar{m}_c$  and  $m_c^w$  is used. Fig. 16 illustrates how well this works for different  $\kappa$ .

The tree-level relation (32) is exact to all orders in  $a^n$ . This is because the mass  $\bar{m}_c$  is the *off-shell* mass, defined at  $q^2 = 0$  in contrast to the pole mass. As promised in the introduction, we never use the pole mass.

Figs. 14 and 16 show the moment ratios of the subtracted correlator as well. The corresponding lines terminate at  $n = 2$ . Again, just like in the case of a single resonance

(Figs. 2,3,4) the second ratio  $r_2$  is affected by the subtraction. The effect is seen to be smaller at smaller values of the fermion mass (higher  $\kappa$ ). The third ratio  $r_3$  is affected very little, while the moment ratios for  $n > 3$  are insensitive to subtractions.

### 3.2 Fit of the lower moments

As explained in the section 1, the correlator of *heavy*-quark currents is special in the way that the lower moments, which originate from the short-distance part of that correlator, are determined by perturbative QCD. The lowest moments must be saturated by one-loop of free quarks. Therefore we fit those moments, obtained by Monte-Carlo on the lattice, with one loop of free Wilson quarks.

In this section we neglect  $\mathcal{O}(\alpha_s)$  terms and obtain an approximate value of the renormalized heavy-quark mass  $\bar{m}_c$  from the ratio  $r_3$ :

$$\bar{m}_c^2 \approx \frac{1}{4} \frac{a_3}{r_3^{lat}} \quad (33)$$

We use the coefficient  $a_3$  of the continuum theory because the coefficients  $a_n$  of the continuum theory (27) - (29) fit the lattice correlator, composed of Wilson propagators, so well (see Fig. 15, 16), provided the mass relation (32) is used.

Fig. 18 shows the fit of Monte-Carlo data at  $n = 3$  by the moments of the pseudoscalar correlator, saturated by one loop of effectively free Wilson quarks. Those quarks are found to have  $\tilde{\kappa} = 0.0994$ , which for free Wilson quarks implies,  $am_c^w = 1.02$  because of eq.(26). From the previous section we know that for such a large mass it is important to correct for the  $\mathcal{O}(a)$  systematic deviation (32). One obtains  $a\bar{m}_c(am_c^w = 1.02) = 0.72$ , which for  $a^{-1} = 1.9 \text{ GeV}$  gives:

$$\bar{m}_c = 1.37 \pm 0.01 \text{ GeV} \quad (34)$$

where the error is associated with the contribution of the high-energy part of the spectrum.

Other channels, such as vector or scalar, are just as good as the pseudoscalar one for the determination of the renormalized quark mass. The ratio  $r_4$  would be also just as good as  $r_3$  to determine  $\bar{m}_c$ , since the relation between  $r_3$  and  $r_4$  is calculable within perturbative QCD. The difference is  $O(\alpha_s)$ -effect. We consider it in section (3.4).

Note, that the relation (32) is derived in the infinite volume. Since we study rather small lattice  $8^3 * 16$  we would like to be more accurate with the finite-volume effects. The moments of the continuum theory (28) agree with the lattice moments (see Fig. 15, 16), computed in a rather large box  $32^4$ . In the mean time one can notice in Fig. 14 that the moments of the small lattices like  $8^3 * 16$  deviate from the asymptotic  $L \rightarrow \infty$  behavior even at small  $n = \{1, 2, 3\}$ . In the next section we take into account this deviation.

### 3.3 The lattice dispersion relation for the fermionic continuum

We have seen on Fig. 15, 16 that the moment ratios  $r_n$  of the lattice correlator in the free-Wilson-quarks approximation follow the corresponding ratios of the continuum theory with the correct value of the quark mass. The moments (27) - (29) of the continuum theory can be calculated with the help of the spectral representation (7) with the spectral density corresponding to one-loop of free quarks. For the three channels under discussion one can use:

$$\rho^{vec}(s) = \frac{1}{4\pi^2} (s + 2(\bar{m}_c)^2) \sqrt{1 - 4(\bar{m}_c)^2/s} \quad (35)$$

$$\rho^{psc}(s) = \frac{3}{8\pi^2} s \sqrt{1 - 4\bar{m}_c/s} \quad (36)$$

$$\rho^{sca}(s) = \frac{3}{8\pi^2} (s - 4(\bar{m}_c)^2) \sqrt{1 - 4(\bar{m}_c)^2/s} \quad (37)$$

We would like to see how well the lattice variant of the dispersion relation (13) works for the continuum spectrum of free fermions. We can use the spectral densities (35) - (37) in the eqn. (13) and compare the result with the correlator composed of free Wilson

propagators. We plot the moment ratios obtained in those two ways on Fig. 17 in the case of small lattice  $8^3 * 16$ . We fit the moments of the lattice correlator of free Wilson fermions with corresponding moments of the correlator computed via the dispersion relation (13) with the spectral density (36). This is a one-parameter fit. That parameter is the quark mass of the continuum theory  $\bar{m}_c$ . We find the agreement illustrated by Fig. 17 remarkable.

Thus, the use of the lattice dispersion relation (13) for the continuum spectrum of quark-antiquark pair helps to fit the moments on small lattices. It appears as an efficient instrument to take into account-finite size effects. On bigger lattices one can simply use the formula (32).

### 3.4 Fixing the subtraction scheme

In this section we estimate the value  $m_c^{MS}(m_c)$  of the renormalized charmed-quark mass in the minimal subtraction scheme normalized at the Euclidean point  $\mu = m_c$ . In order to fix the subtraction scheme one should be sensitive to the  $\alpha_s$ -correction in the ratios  $r_n$ . The study of the systematic deviations of the coefficient  $b_n$  is beyond the framework of the present paper. However, since the term  $b_n \alpha_s$  is small in the lower ratios  $r_{2,3,4}$  we will take its values from the continuum theory. This is our approximation. To be more precise, we write the lower ratios as

$$\begin{aligned}
 r_n &= \frac{a_n}{4m_c^2} \xi_n \\
 \xi &\equiv 1 + \alpha_s b_n/a_n
 \end{aligned}
 \tag{38}$$

We take the value of the strong coupling constant  $\alpha_s(m_c) \approx 0.3$ <sup>2</sup>. Based on the two-loop calculations of the continuum theory [10] we obtain for the vector, pseudoscalar and scalar

<sup>2</sup>To fix precisely the normalization point of  $\alpha_s$  in every moment one needs to know the three-loop correction in the ratios (10), which is not known at present

channels:

$$\begin{aligned}\xi_3^{psc} &= 1.02, & \xi_3^{vec} &= 0.95, & \xi_3^{sca} &= 0.97 \\ \xi_4^{psc} &= 0.96, & \xi_4^{vec} &= 0.92, & \xi_4^{sca} &= 0.91\end{aligned}\tag{39}$$

The  $\alpha_s$ -term is seen to introduce a few-percent correction to the ratios  $r_{2,3,4}$ . Therefore, the presently unknown cutoff effects in the coefficient  $b_n$  have a small effect on the value of the quark mass  $\bar{m}_c$ .

We fit the lower moment ratios  $r_{3,4}$  of our Monte-Carlo data using the lattice spectral representation, as explained in the previous section, to relate more accurately the quark mass of the continuum theory  $\bar{m}_c$  to the corresponding Wilson propagator in the finite-volume lattice theory.

The results for the renormalized charmed-quark mass are shown in the tables. The tables demonstrate that the dimensionless ratio of the renormalized quark mass to the resonance mass  $\bar{m}_c/m_{res}$  is very stable with respect to significant variation of  $\kappa$ . This implies that the renormalized heavy-quark mass is less sensitive to the uncertainty in the value of the lattice spacing than one might expect.

The relation  $\bar{m}_c[\kappa, \beta]$  between the renormalized heavy-quark mass and bare parameters of the lattice theory is, in principle, rather non-trivial. On Fig. 18 we plot the moments of one loop of the free Wilson quarks with the input  $\kappa = 0.1060$  (dashed line) to show how different they are from the moments of one loop of free quarks with  $\tilde{\kappa}$  corresponding to the renormalized mass (bottom line). At large values of  $\beta$  the relation between  $\kappa$  and  $\tilde{\kappa}$  is perturbative. We have generated 20 gauge configurations for  $\beta = 20$  with the same Monte-Carlo parameters as for  $\beta = 6$ . The corresponding moments of the correlator with the clover-and-tadpole-improved propagators for the same input  $\kappa = 0.1060$  are shown on Fig. 18 by squares. The Monte-Carlo data for  $\beta = 20$  is fitted perfectly at all  $n$  by one loop of free-quarks (upper solid line) with  $\kappa' = 0.1034$ . We find numerically the

relation :

$$\kappa' = \kappa < U_{\square}(\beta = 20) >^{1/4} \quad (40)$$

Obviously the data at  $\beta = 20$  shows the correlator at distances so small that the effects due to interaction are not seen. The contribution of the clover term is strongly suppressed. The relation (40) is due to the fact that we used the mean-field-tadpole-improved action [16]. Generating the correlator by Monte-Carlo at various high values of  $\beta$  one can study the correlator in the weak-coupling expansion [14].

## 4 Conclusions

We have formulated in details the way to calculate the renormalized quark mass using Monte-Carlo data on the correlator of heavy-quark currents. We separate the long-distance and the short-distance parts of the correlator by studying the higher and the lower moments of the correlator respectively. The long-distance part is used to fix the scale of the lattice theory, as it is saturated by the lowlying resonance. The short-distance part is fitted by the loop expansion of perturbative QCD. The coefficients of that expansion are contaminated by the cutoff effects and the finite-volume effects. Those systematic deviations can be studied order by order in the loop-expansion. We have worked out systematic deviations of the one loop of Wilson quarks, which saturates the very short-distance part of the correlator (the lowest moments). Then fit to Monte-Carlo data produces the value of the renormalized heavy-quark mass. We find for the charmed quark mass:  $m_c^{\overline{MS}}(m_c) = 1.22(2)GeV$  - from the vector channel and  $m_c^{\overline{MS}}(m_c) = 1.18(2)GeV$  - from the pseudoscalar channel. There are two sources of uncertainties in these values. The first is the ansence of scaling on the present lattice. The data for higher  $\beta > 6$  as well as improved actions should helpful in this respect. The second uncertainty is in fixing the

scale. One needs bigger volume to determine the resonance mass with better accuracy. The dimensionless ratio of the renormalized heavy-quark mass to the resonance mass is stable with respect to variation of  $\kappa$  provided the value of  $\kappa$  corresponds to heavy quarks.

Our central value for the charmed quark mass in the vector channel can be compared to the corresponding estimate of the continuum theory :  $m_c^{\overline{MS}}(m_c) = 1.23\text{GeV}$  [2]. There are no estimates of the charmed quark mass from the pseudoscalar or scalar correlators in the continuum theory, since the corresponding spectral densities are not observable experimentally.

A comprehensive study of the correlator of heavy-quark currents at both large and small distances is a challenging problem. One principal question we tried to clarify here is whether one can observe simultaneously, on the lattice sizes presently available to Monte-Carlo simulations, both short-distance phenomena, described by asymptotic freedom, and long-distance tails of hadronic correlators, saturated by low-lying resonances. In order to see short-distance phenomena one has to keep the lattice spacing small. Then one needs many lattice sites in order to reach large physical scales, where the low-energy part of the hadronic spectrum dominates. To solve this problem it is crucial to combine the extension of dispersion relations to the lattice with the improved actions. The former helps to fit correlators in smaller volumes, while the latter helps to see QCD perturbation theory on coarse lattices. Further study of the  $\alpha_s$ -corrections [14] to the correlator of the heavy-quark currents on the lattice is necessary to specify the renormalization scheme of the extracted quark mass more accurately and measure the renormalized strong coupling constant.

## Acknowledgments

One of the authors (A. B.) would like to thank P. van Baal, P. Lepage, L. McLerran, J. Kapusta, A. Kovner, M. Shifman, J. Smit, A. Vainshtein, M. Voloshin, R. Willey for useful discussions and DOE for support under the grant DE-FG02-87ER40382. We thank the QCD-TARO collaboration for generating the blocked  $SU(3)$  configurations we used. Computer time for this project was provided by the Minnesota Supercomputer Institute and by the Pittsburgh Supercomputer Center.

## References

- [1] For a review see: S. Bethke, in : Nucl. Phys. Proc. Suppl. 39 (1995).
- [2] For a review see: S. Narison, *A fresh look into the heavy-quark mass values*, Preprint CERN-TH 7405/94.
- [3] F. Yndurain, Phys. Rev. D51 (1995) 6348.
- [4] A. El-Khadra et. al., Phys. Rev. Lett. 69 (1992) 729.
- [5] C. Davies et. al., Phys. Rev. D 50 (1994) 6963.
- [6] L. Karsten, J. Smit, Nucl. Phys. B 183 (1981) 103.
- [7] A. Gonzalez Arroyo, F. Yndurain, G. Martinelli, Phys. Lett. B117 (1982) 437.
- [8] C. Allton et. al., Nucl. Phys. B 431 (1994) 667.
- [9] A. Bochkarev, Nuclear Physics B. Proc. Suppl. 42 (1995) 219.
- [10] M. Shifman, A. Vainshtein, V. Zakharov Nucl. Phys. B 147 (1979) 385, 448.
- [11] V. Novikov et. al. Nucl. Phys. B 249 (1985) 445.



- [12] A. Di Giacomo, G. Rossi Phys. Lett. B 100 (1981) 481;  
A. Di Giacomo, G. Paffuti Phys. Lett. B 108 (1982) 327.
- [13] K. Chetyrkin, N. Krasnikov, A. Tavkhelidze, Phys. Lett. B 76 (1978) 83.
- [14] A. Bochkarev, Ph. de Forcrand, In preparation.
- [15] QCD-TARO Collaboration, Phys. Rev. Lett. 71 (1993) 3063.
- [16] P. Lepage, P. Mackenzie Phys. Rev. D 48 (1993) 2250.
- [17] G. Bali, K. Schilling, Phys. Rev. D 46 (1992) 2636.
- [18] A. Borici and Ph. de Forcrand, Nuclear Physics B. Proc. Suppl. 42 (1995) 309.
- [19] B. Sheikholeslami, R. Wohlert, Nucl. Phys. B 259 (1985) 572.
- [20] G. Martinelli, C. Sachrajda, A. Vladikas, Nucl. Phys. B358 (1991) 212.
- [21] C. Allton, et al., Phys. Lett. B292 (1992) 408; A. El-Khadra, Nucl. Phys. B (Proc. Suppl.) 30 (1993) 449.

fit to $r_3$	$m_{res}$	$\bar{m}_c$	$\bar{m}_c/m_{res}$	$m_c^{\bar{M}S}[a_{J/\psi}]$	$m_c^{\bar{M}S}[a_{\eta_c}]$
$\eta_c$	2.024(9)	.779(2)	.385	1.18	1.16
$J/\psi$	2.06(1)	.835(2)	.406	1.23	1.20
$\chi_o$	2.29(12)	.778(9)	.340	1.15	1.13
fit to $r_4$	$m_{res}$	$\bar{m}_c$	$\bar{m}_c/m_{res}$	$m_c^{\bar{M}S}[a_{J/\psi}]$	$m_c^{\bar{M}S}[a_{\eta_c}]$
$\eta_c$	2.024(9)	.815(2)	.403	1.20	1.18
$J/\psi$	2.06(1)	.861(3)	.418	1.24	1.22
$\chi_o$	2.29(12)	.827(10)	.361	1.19	1.16

Table 1. Charm-quark mass as a result of the fit of the ratios  $r_3$ ,  $r_4$  of the subtracted correlator for  $\kappa = 0.1000$ . The masses  $m_{res}$  and  $\bar{m}_c$  are in units of the lattice spacing. The masses  $m_c^{\bar{M}S}[a_{J/\psi}]$  and  $m_c^{\bar{M}S}[a_{\eta_c}]$  are in  $GeV$ . They are obtained assuming that the lattice spacing is fixed from the vector channel and from the pseudoscalar channel respectively. The indicated errors are statistical.

fit to $r_3$	$m_{res}$	$\bar{m}_c$	$\bar{m}_c/m_{res}$	$m_c^{\bar{M}S}[a_{J/\psi}]$	$m_c^{\bar{M}S}[a_{\eta_c}]$
$\eta_c$	1.565(1)	.596(2)	.381	1.16	1.15
$J/\psi$	1.61(2)	.651(4)	.404	1.22	1.21
$\chi_o$	1.87(10)	.609(9)	.326	1.15	1.14
fit to $r_4$	$m_{res}$	$\bar{m}_c/m_{res}$	$\bar{m}_c$	$m_c^{\bar{M}S}[a_{J/\psi}]$	$m_c^{\bar{M}S}[a_{\eta_c}]$
$\eta_c$	1.57(1)	.623(3)	.398	1.17	1.16
$J/\psi$	1.61(2)	.666(4)	.414	1.23	1.22
$\chi_o$	1.87(10)	.649(10)	.347	1.19	1.18

Table 2. The same as in Table 1 for  $\kappa = 0.1060$ .

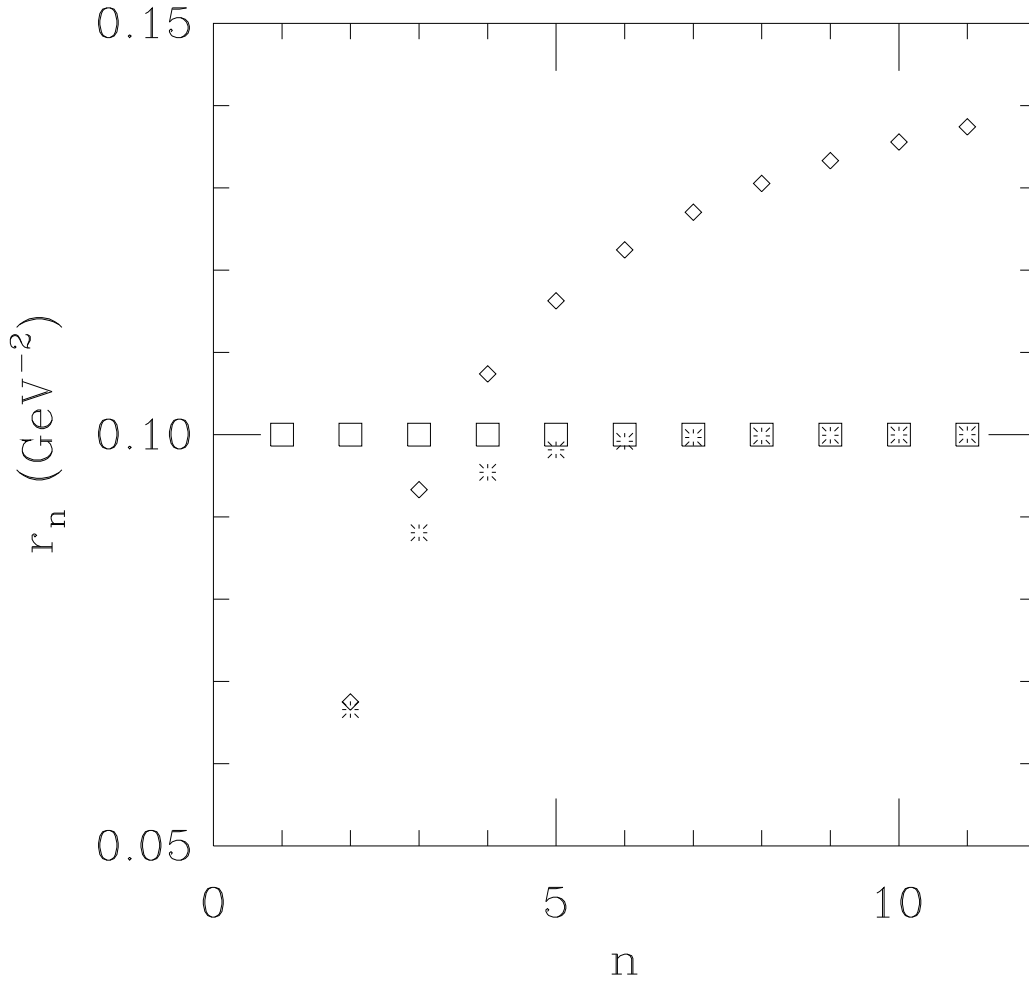


Figure 1: Ratios of the neighboring moments in the continuum theory for the correlator of interpolating currents of the  $J/\psi$ -meson. Burst symbols correspond to the evaluation of the correlator via dispersion relation with the phenomenological hadronic spectrum (11). Squares show the contribution of a single  $J/\psi$ -resonance. Diamonds are moments of one loop of free quarks with mass  $m_c = 1.26 \text{ GeV}$ .

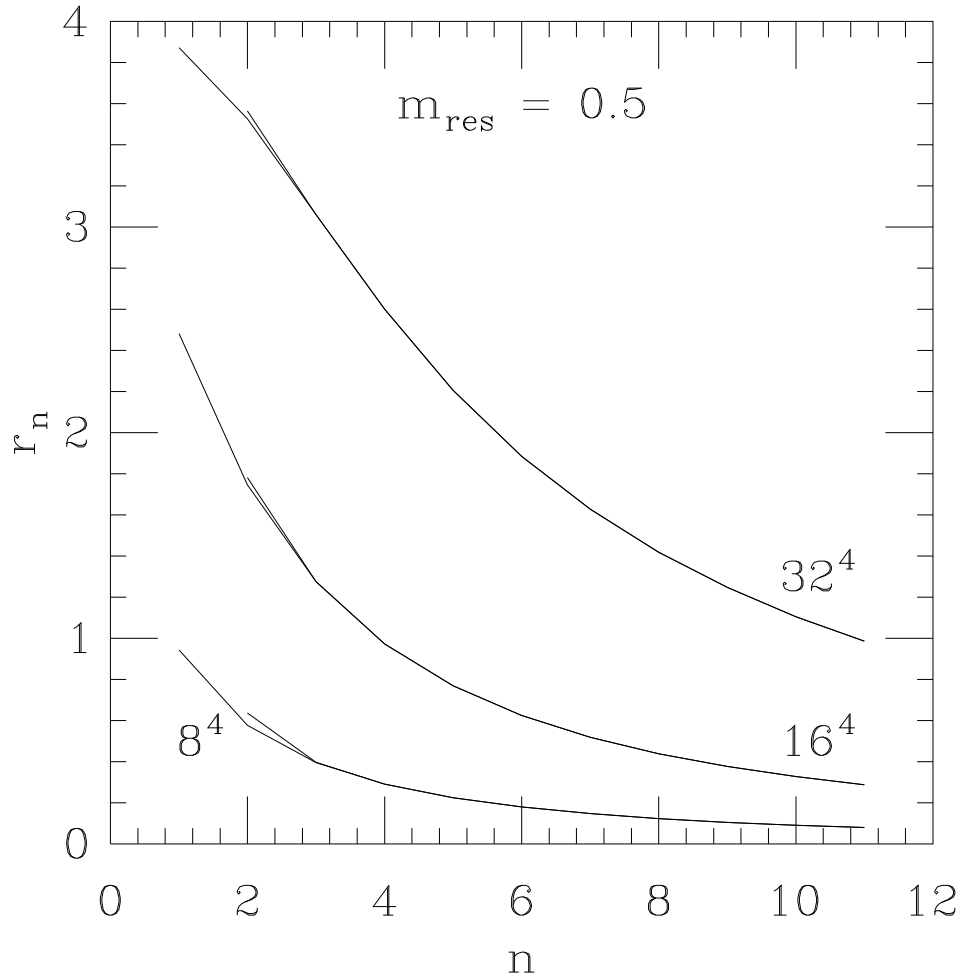


Figure 2: Ratios of the neighboring moments of the single resonance approximation to the correlator, on three lattices of different sizes:  $8^4$ ,  $16^4$ ,  $32^4$ . The resonance mass ( $m_{res} = 0.5$ ) is given in the units of the inverse lattice spacing. Solid lines are to guide the eye. The lines becomes double near  $n = 2$ : then one line corresponds to the subtracted correlator (terminating at  $n = 2$ ), the other - to the unsubtracted one.

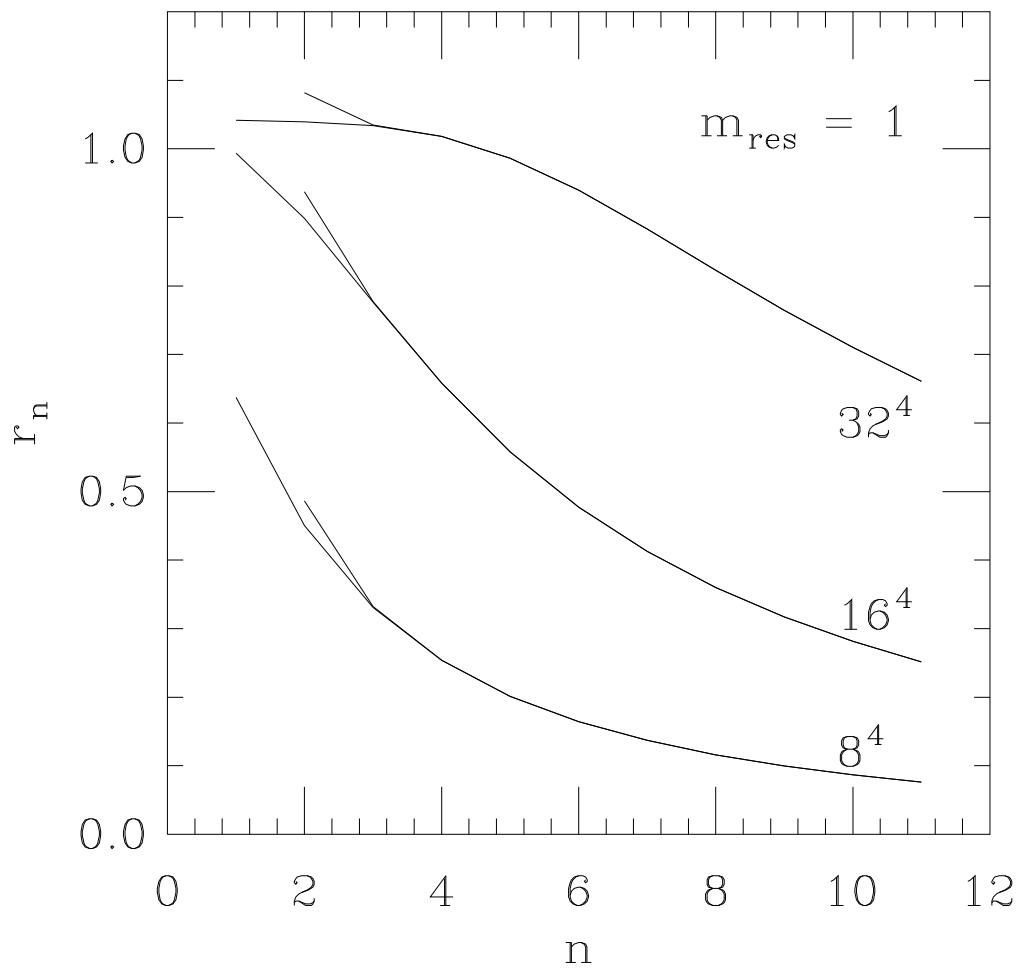


Figure 3: Same as in Fig.2, for  $m_{res} = 1$ .

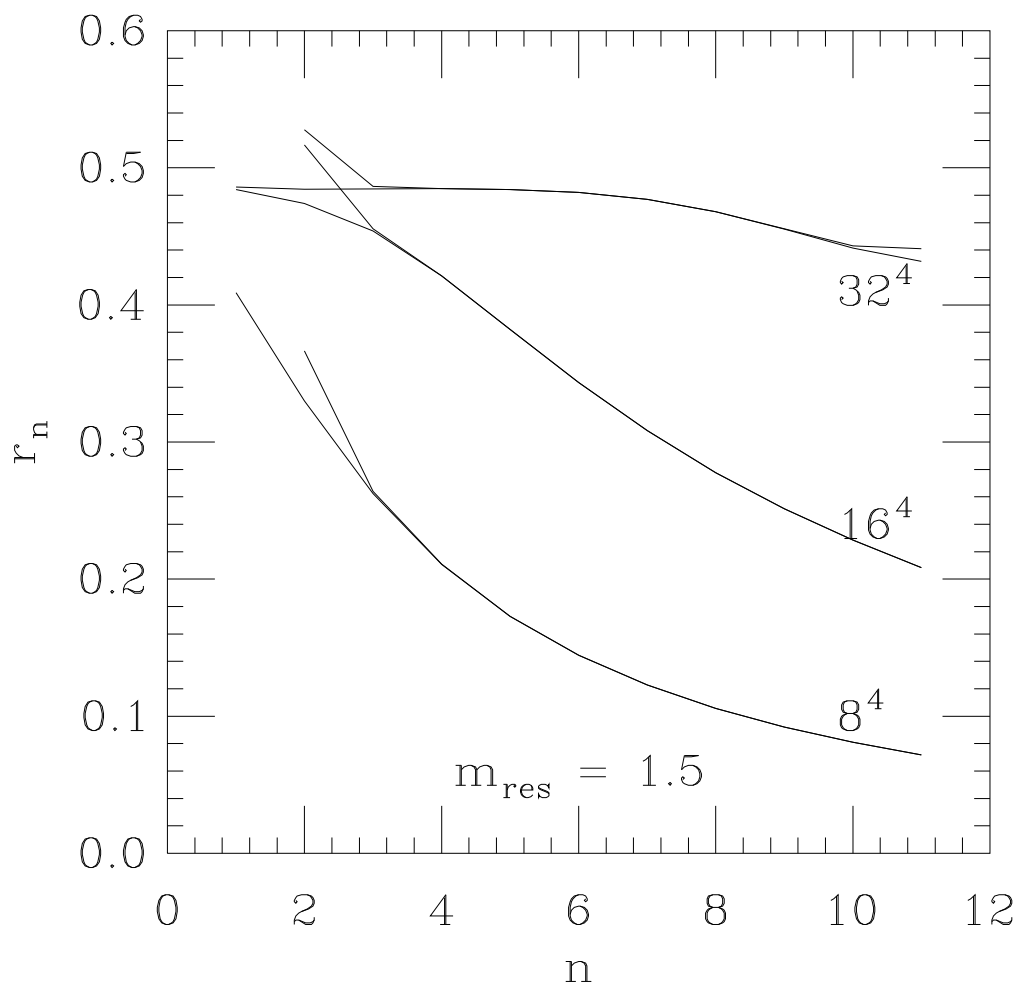


Figure 4: Same as in Fig.2, for  $m_{res} = 1.5$ .

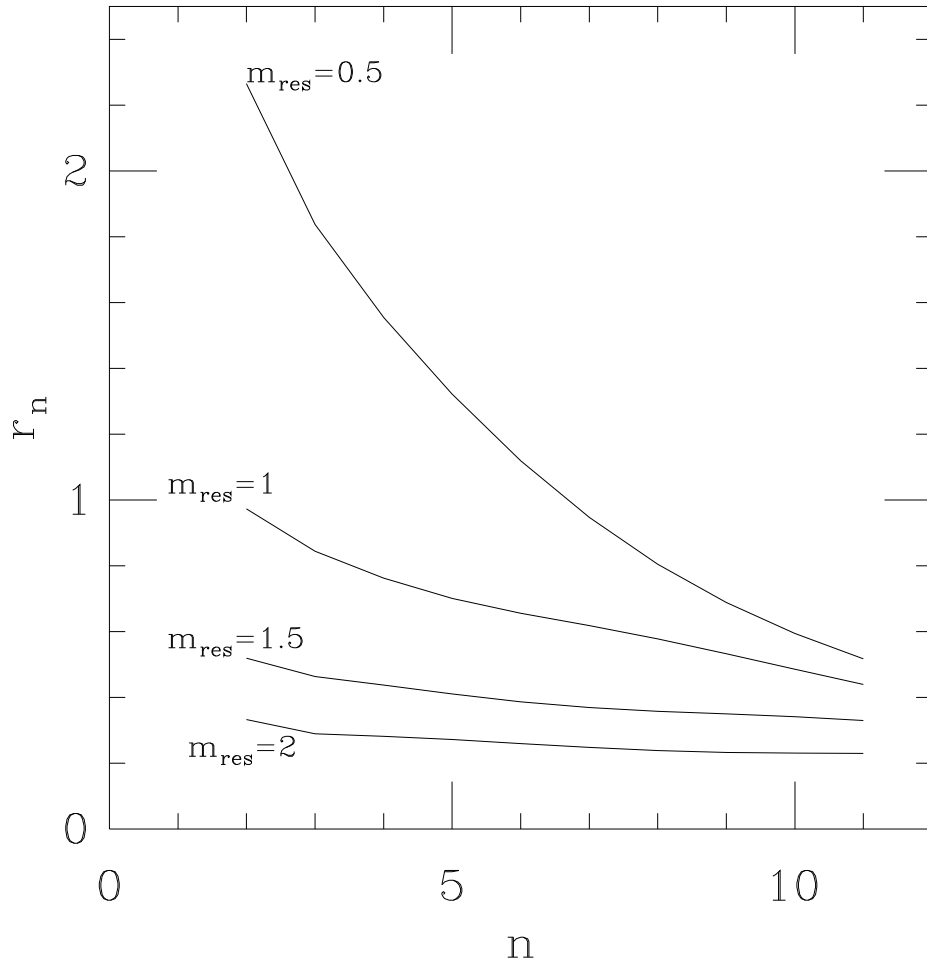


Figure 5: Resonance-mass dependence of the ratios  $r_n$  of a single resonance on the lattice  $16^3 \times 32$ .



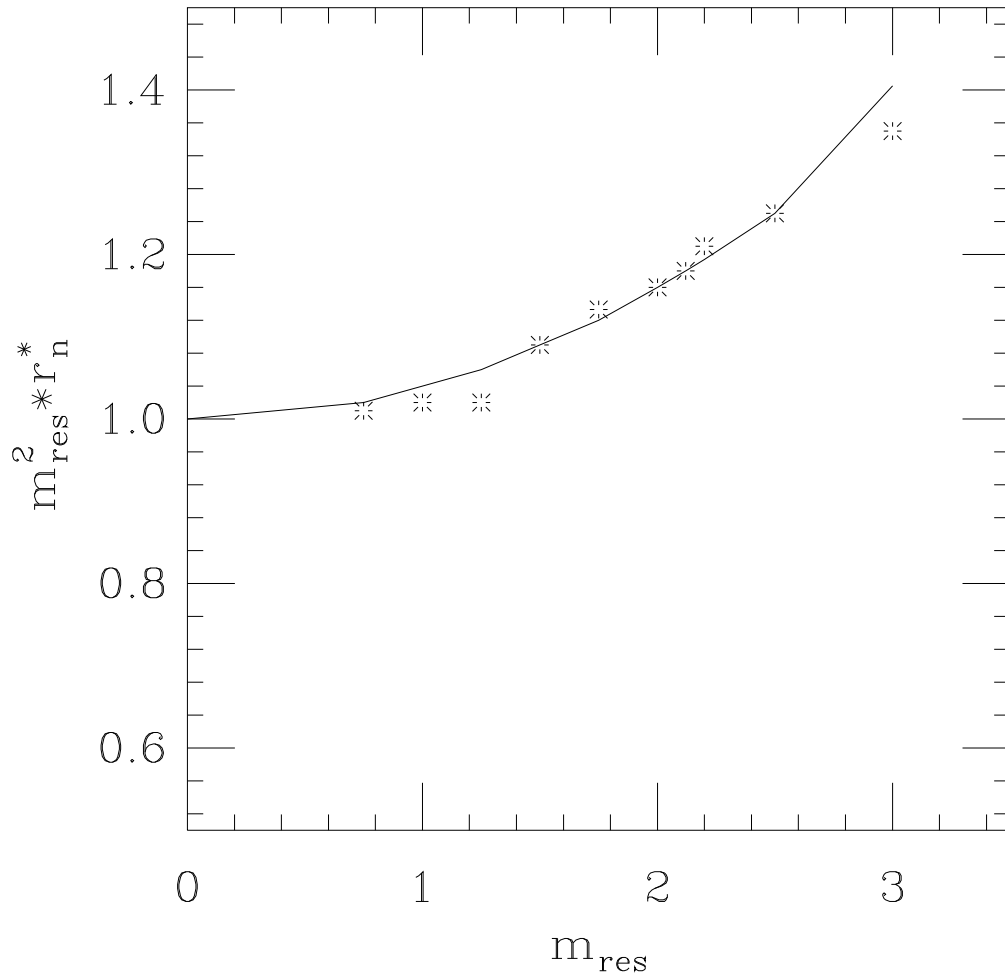


Figure 6: Systematic deviation  $\mathcal{O}((am_{\text{res}})^2)$  of the resonance mass  $\bar{m}_{\text{res}}$ , extracted from the ratios  $r_n$  as a function of the input resonance mass  $m_{\text{res}}$ . The solid line is the fit:  $1 + 0.04m_{\text{res}}^2$ .

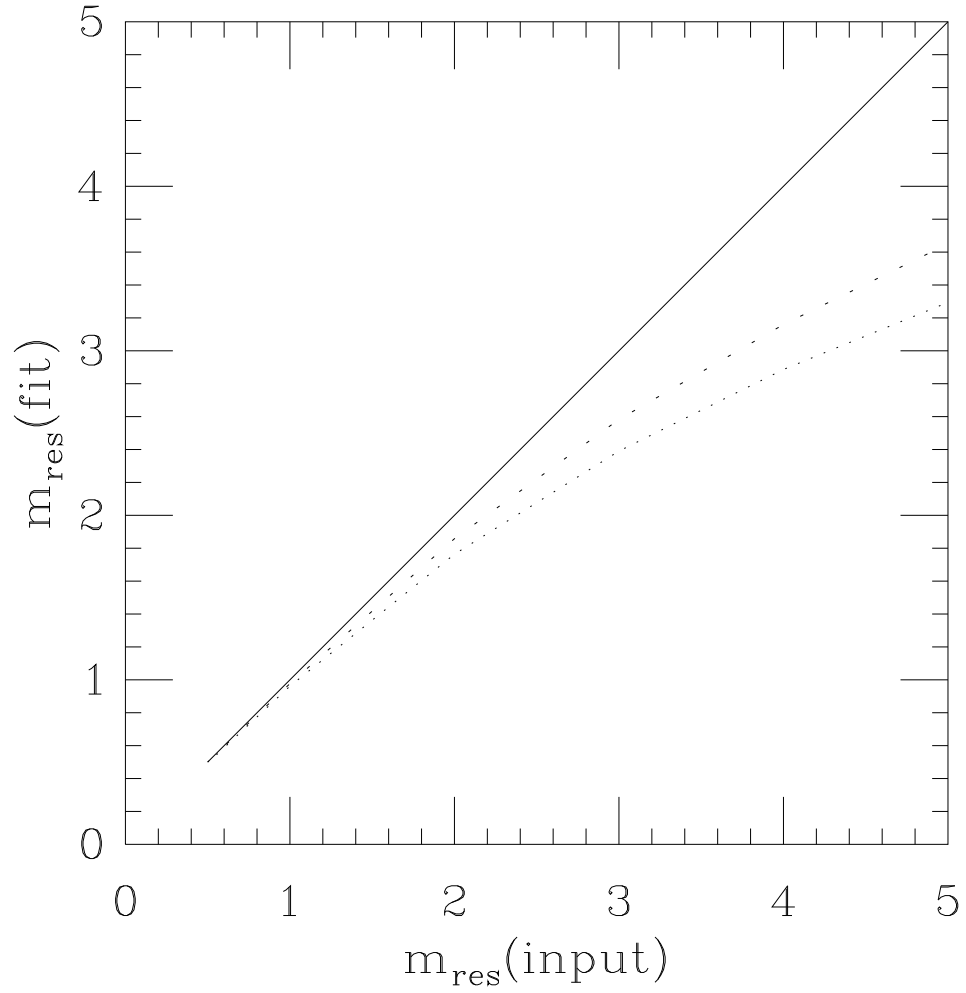


Figure 7: Systematic deviation  $\mathcal{O}((am_{\text{res}})^2)$  of the resonance mass, extracted in two different ways: the dotted line is a conventional fit of the zero-momentum correlator to  $\cosh[(t-L/2)m_{\text{res}}]$ ; the dashed line is the resonance mass obtained from the ratios  $r_n$ .

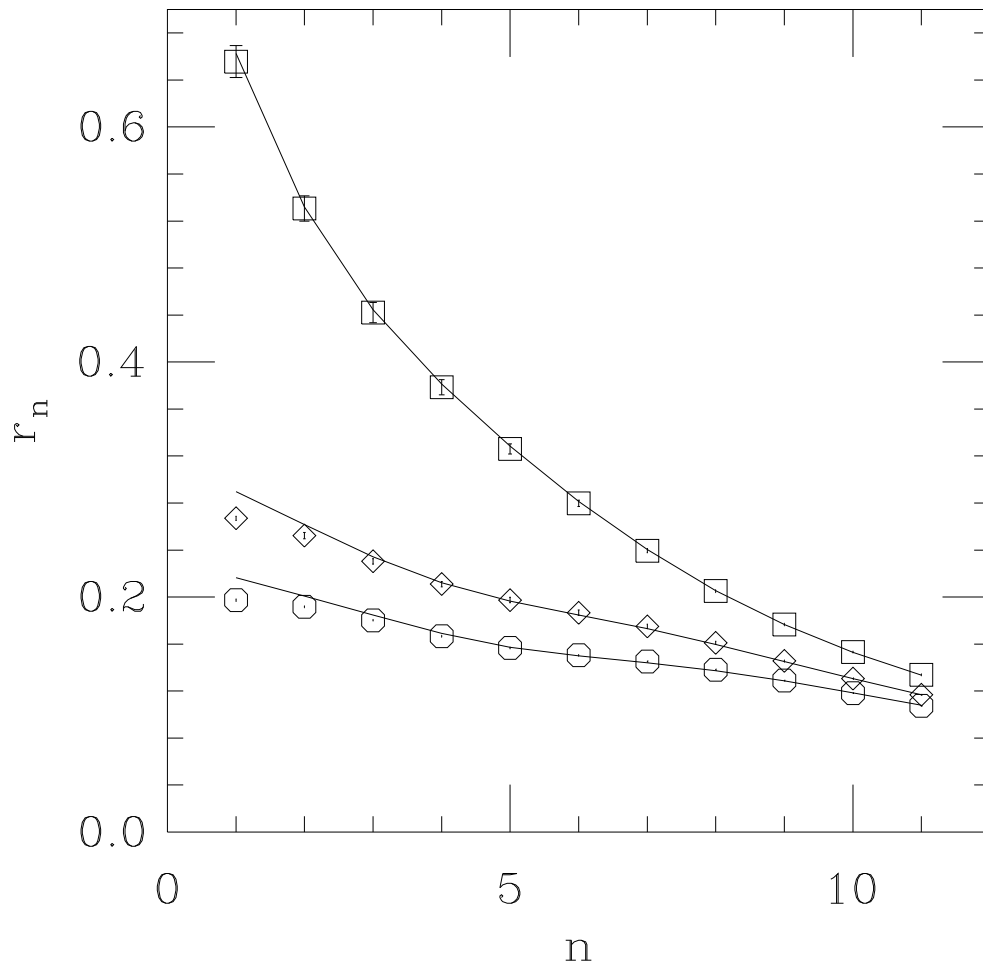


Figure 8: Ratios  $r_n$  of the Monte-Carlo data for the pseudoscalar currents on the lattice  $8^3 \times 16$ , blocked from  $32^3 \times 64$ ,  $\beta = 6$ . Solid lines show the one-parameter ( $m_{res}$ ) fit by the ratios of a single resonance. Three sets of data correspond to  $\kappa = \{0.1111, 0.1031, 0.0983\}$ .

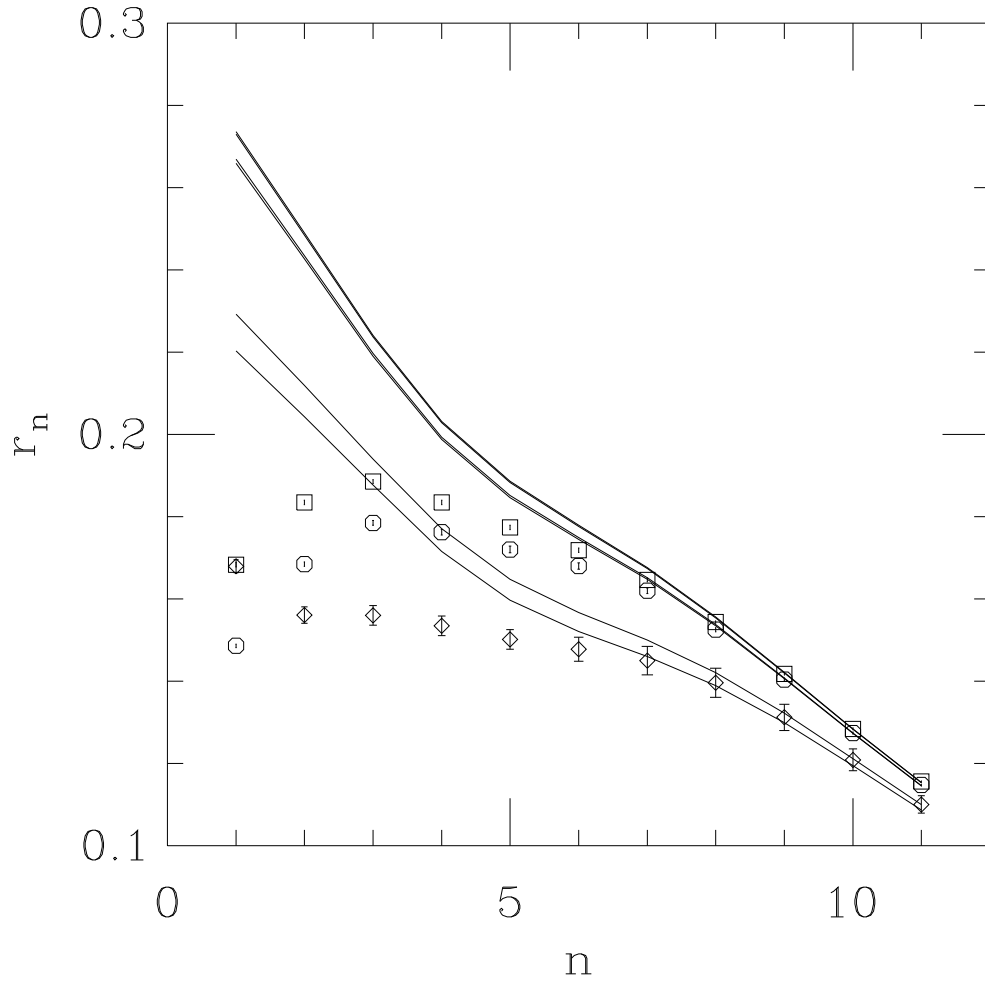


Figure 9: Monte-Carlo data on the  $8^3 \times 16$ ,  $\beta = 6$  - lattice for pseudoscalar (squares), vector (octagons) and scalar (diamonds) currents.  $\kappa = 0.1000$ . Solid double lines show the ratios of a single resonance, whose mass is fitted to the higher ratios. Double lines reflect statistical errors.

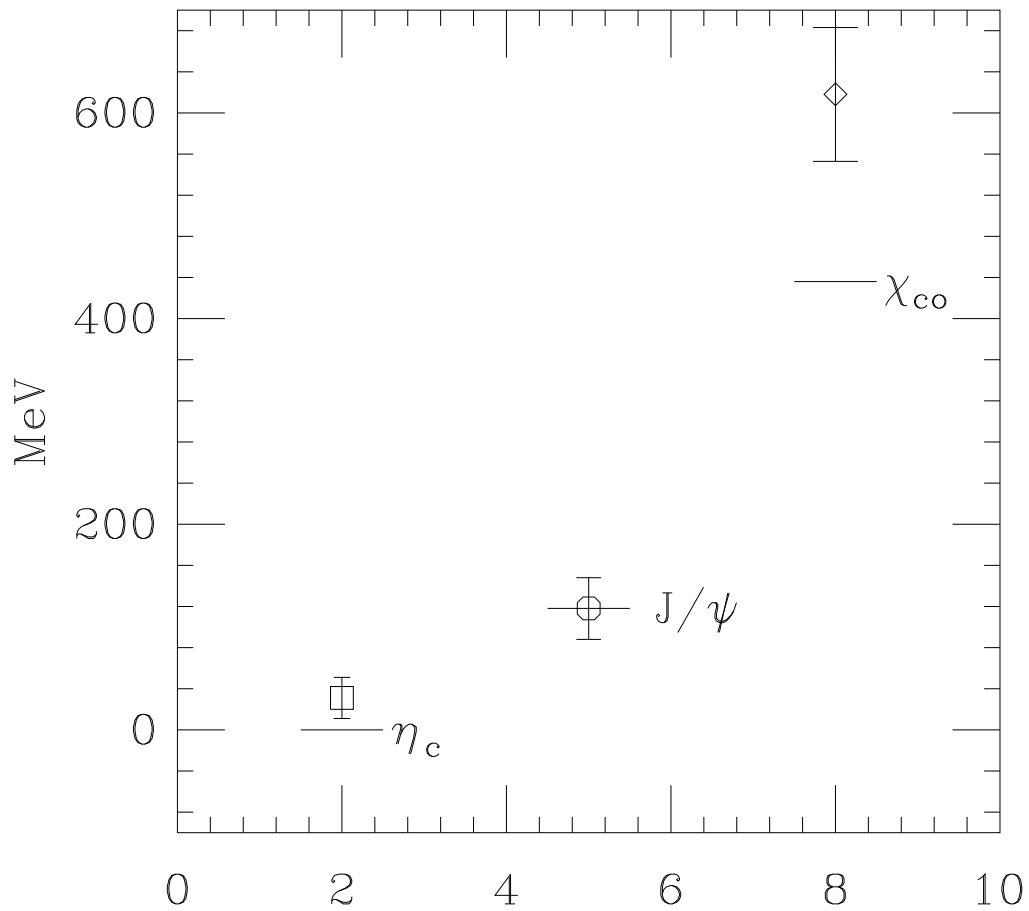


Figure 10: Charmonium spectrum obtained on the  $8^3 \times 16$ -lattice at  $\beta = 6$  with the clover-and-tapole-improved action. The vector mass  $m_{J/\psi} = 3.097 GeV$  is used for normalization. The wide horizontal lines are experimental points.

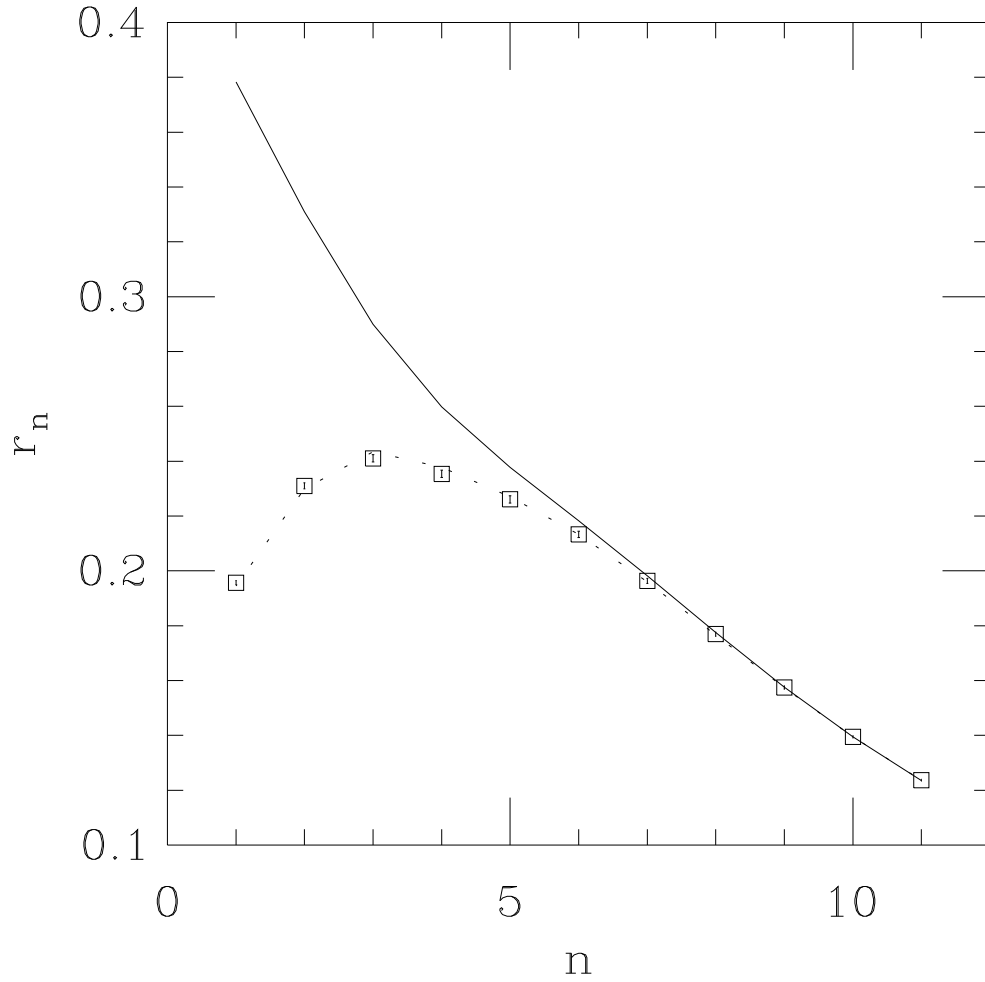


Figure 11: Monte-Carlo data on the  $8^3 \times 16$ ,  $\beta = 6$  - lattice for vector currents,  $\kappa = 0.1060$ . The solid line is a single resonance approximation. The dashed line is the correlator with the phenomenological charmonium spectrum (11) incorporated via the dispersion relation (13).

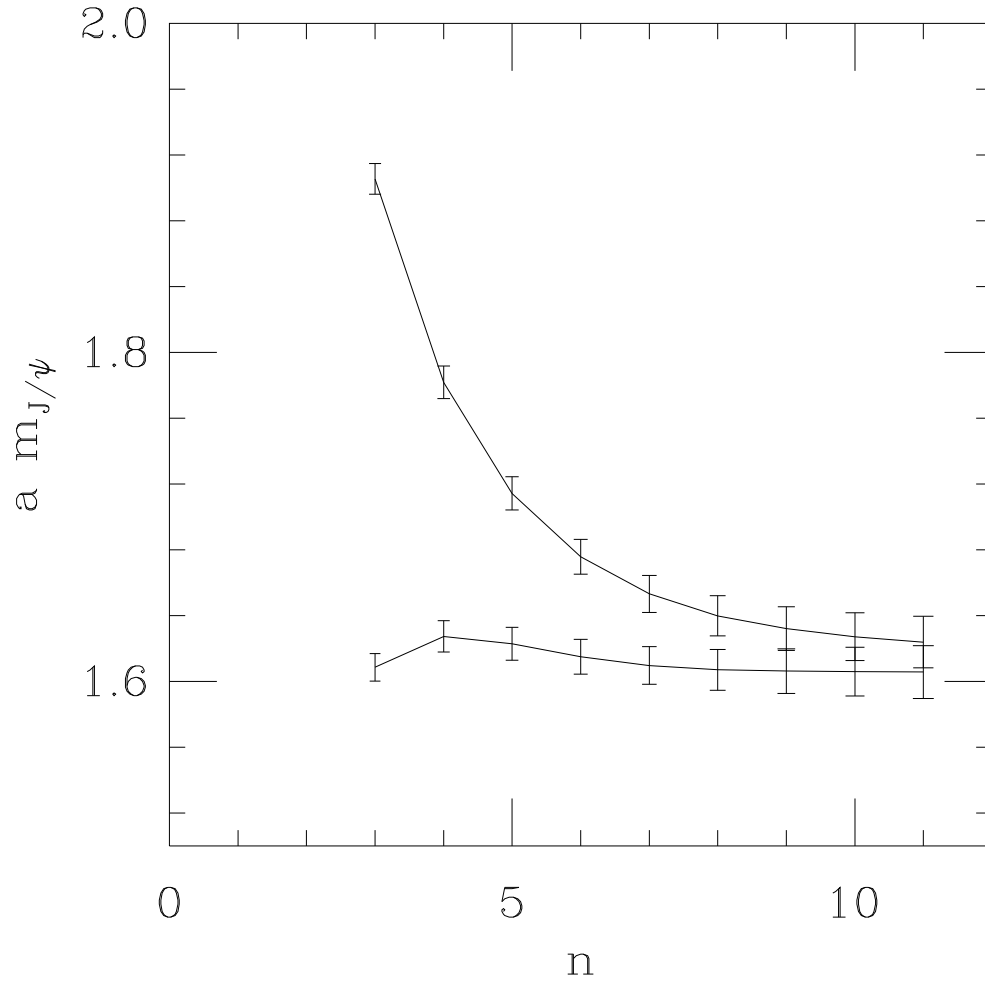


Figure 12: Resonance mass from the fitting the moment ratios of the Monte-Carlo data on the  $8^3 \times 16$ ,  $\beta = 6$  - lattice for vector currents,  $\kappa = 0.1060$ . The upper line is a single resonance approximation. The bottom line corresponds to the correlator with the spectrum of eqn. (5) incorporated via the dispersion relation (13). The residue of the resonance  $f$  and the ratio  $s_o/m_{res}^2$  are kept fixed and taken to have phenomenological values (11) while the resonance mass is a fit parameter.

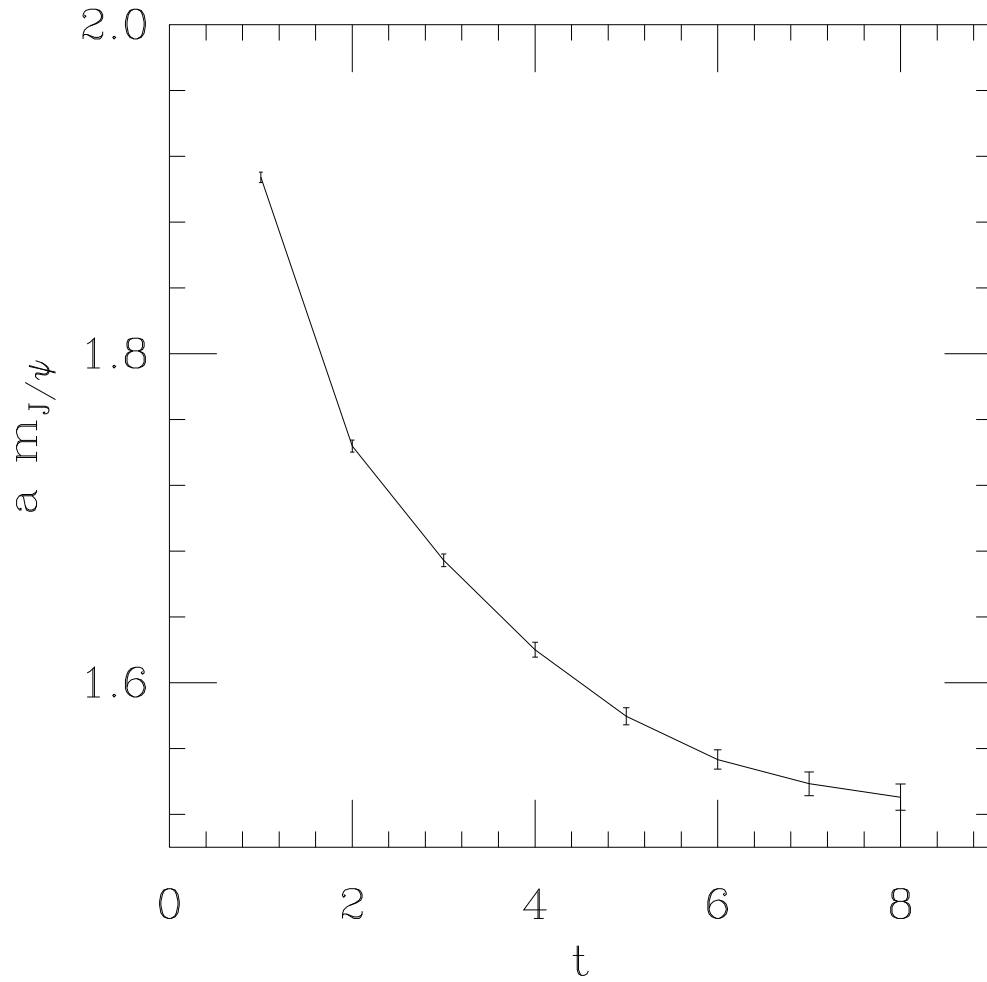


Figure 13: Resonance mass from the conventional fit of the sero-momentum component of the correlator of vector currents (the same Monte-Carlo data as in Fig. 12) to  $\cosh[(t - L/2)m_{res}]$ .



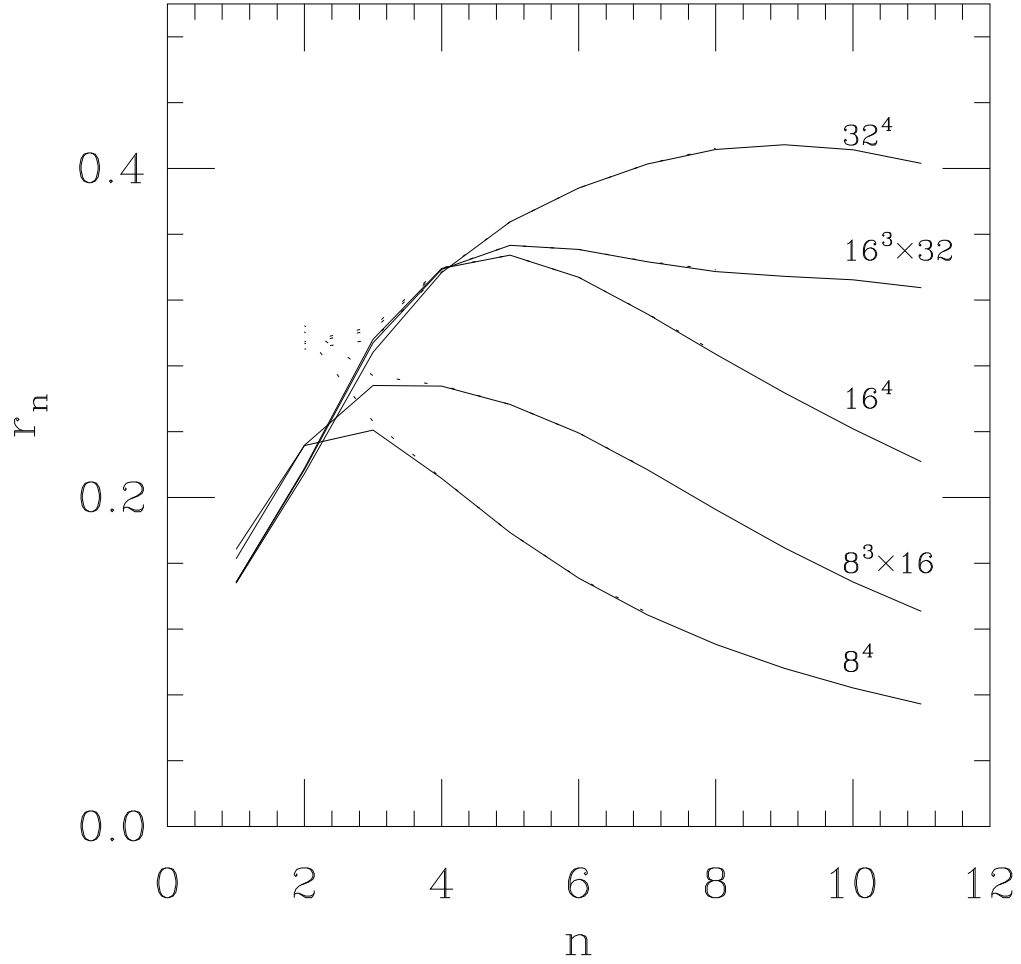


Figure 14: Ratios of the neighboring moments of the subtracted (dashed lines) and unsubtracted (solid lines) correlator of pseudoscalar currents, saturated by one loop of free Wilson fermions with  $\kappa = 0.1$  ( $am_c^w = 1$ ) and periodic boundary conditions, computed numerically on lattices of the indicated size. Lines connect the data to guide the eye.

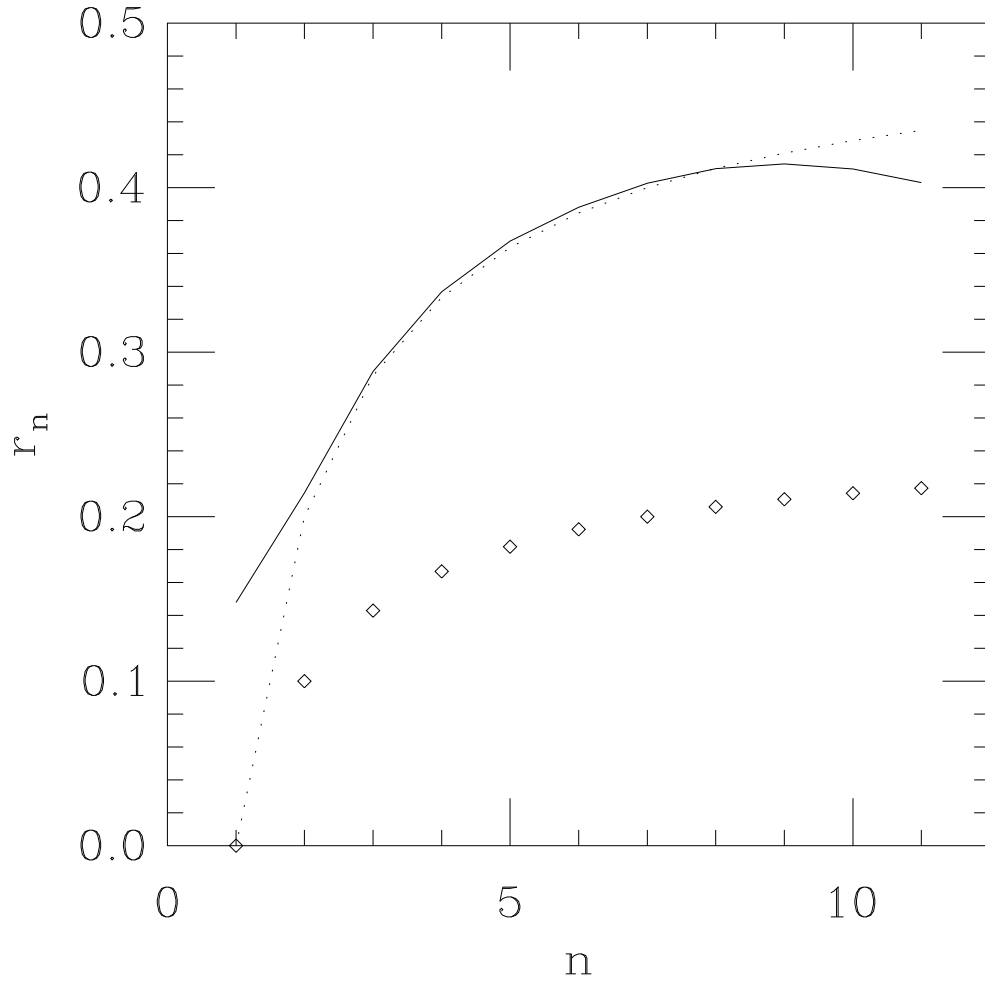


Figure 15: Ratios  $r_n$  for one loop of free Wilson fermions (pseudoscalar currents), computed numerically on the lattice  $32^4$  (solid line) for  $m_c^w$  ( $\kappa = 0.1$ ). Diamonds are the ratios of the continuum theory for  $m_c^w = 1$ . The dashed line shows the ratios of the continuum theory with the corrected mass  $\bar{m}_c$ .

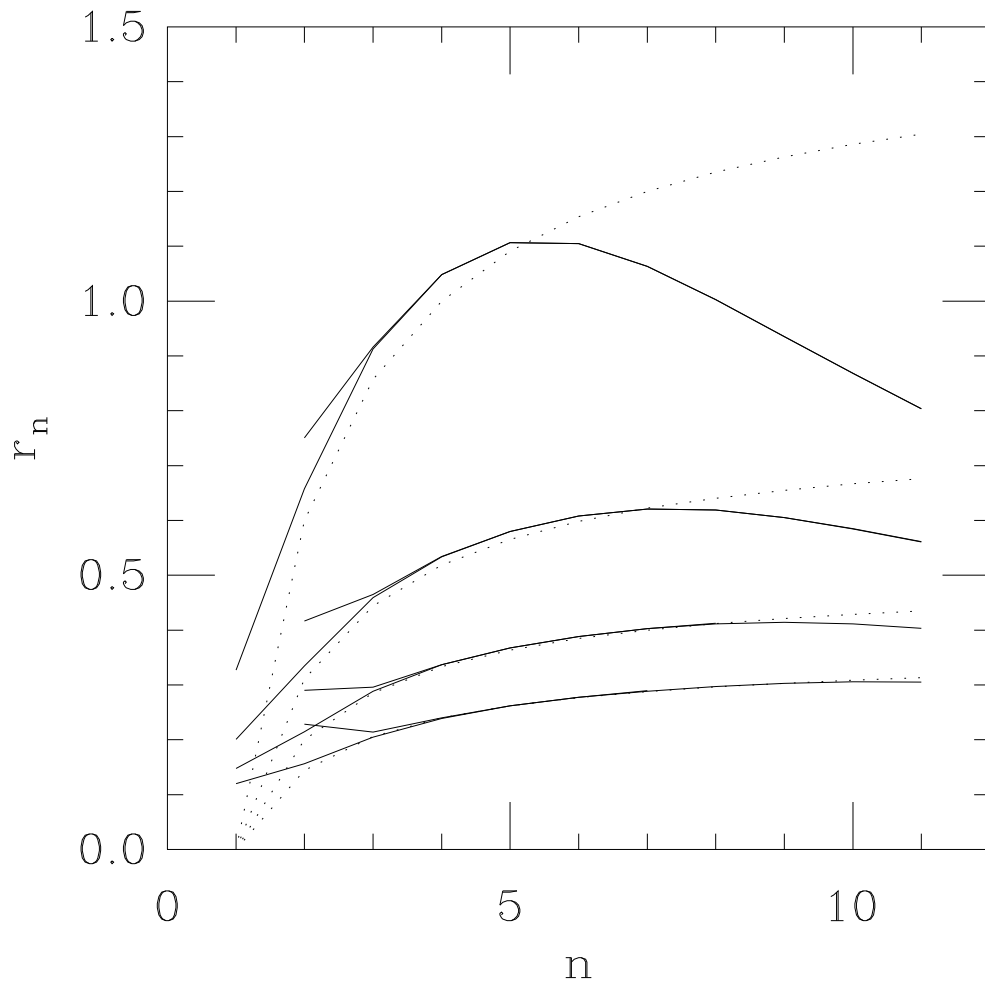


Figure 16: Same as in Fig.9, for  $\kappa = \{0.1111, 0.1053, 0.1, 0.0952\}$ , corresponding to  $m_c^w = \{0.5, 0.75, 1, 1.25\}$ .

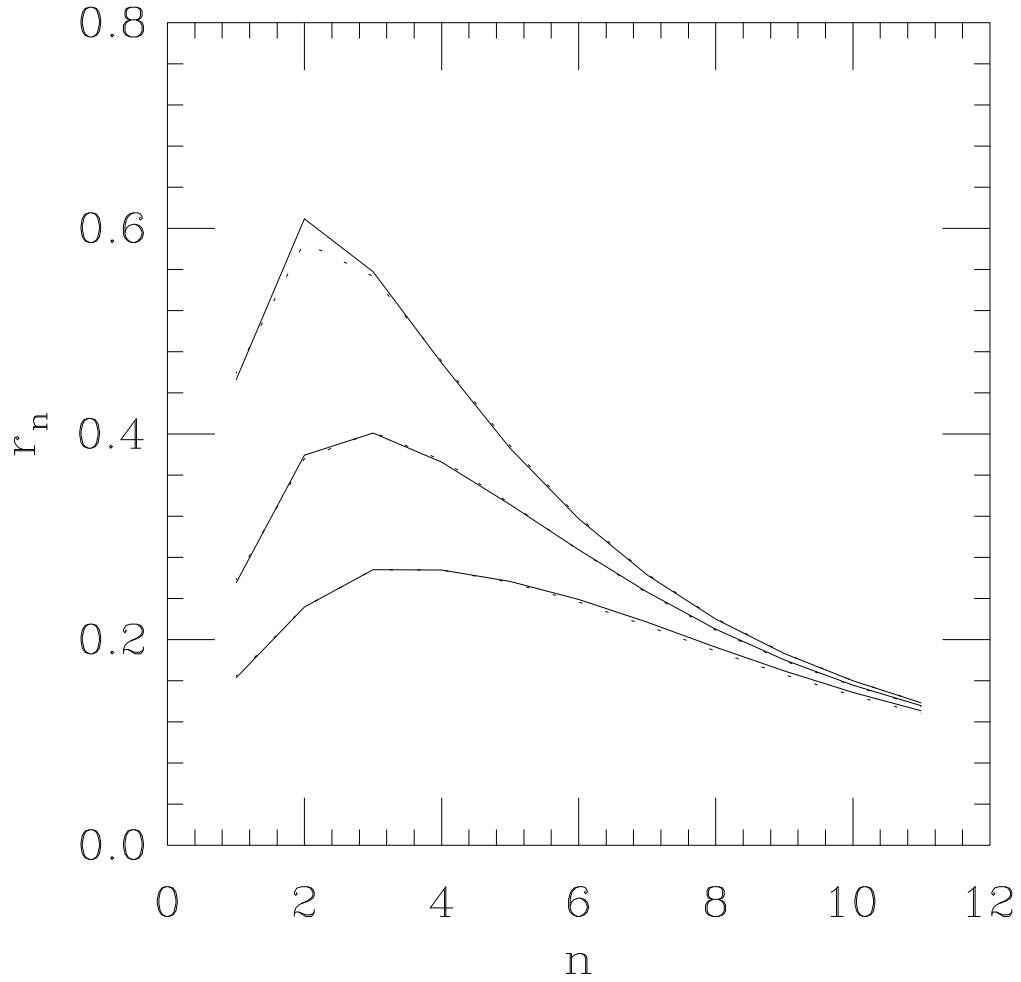


Figure 17: Fit of the pseudoscalar correlator of free Wilson quarks (solid line) with the dispersion relation (dashed line) for  $\kappa = \{0.1111, 0.1060, 0.1000\}$ , corresponding to  $am_c^w = \{0.5, 0.72, 1\}$ .

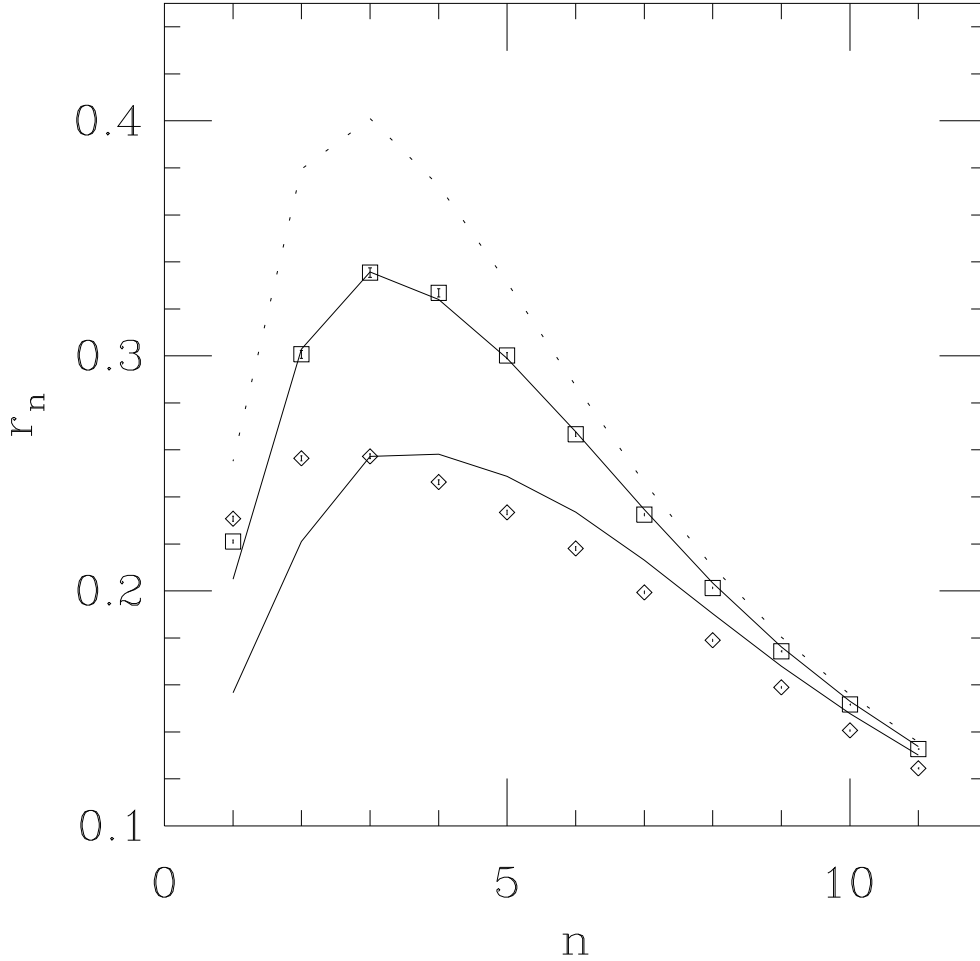


Figure 18: Monte-Carlo data for the pseudoscalar currents on the  $8^3 \times 16$ -lattice at  $\beta = 6$  (diamonds),  $\beta = 20$  (squares);  $\kappa = 0.1060$ . The dashed line shows the ratios for one loop of free Wilson fermions with  $\kappa = 0.1060$ . The solid lines show the ratios for one loop of free Wilson fermions: the bottom solid line is for  $\tilde{\kappa} = 0.0994$ , corresponding to the physical quark mass  $\bar{m}_c = 1.37 GeV$ , the top one is for one loop of Wilson fermions with  $\kappa' = 0.1034 = \kappa < U_{\square}(\beta = 20) >^{1/4}$ .